AFCRL- 67-0421

Monte Carlo Calculations of Light Scattering From Clouds

Authors

Gilbert N. Plass and George W. Kattawar

Southwest Center for Advanced Studies
Dallas, Texas

Contract No. AF19(628)-5039

Project No. 4076

Task No. 407604

Scientific Report No. 2

23 May 1967

This research was partially supported by the National Aeronautics and Space Administration

Prepared
for

AIR FORCE CAMBRIDGE RESEARCH LABORATORIES
OFFICE OF AEROSPACE RESEARCH
UNITED STATES AIR FORCE
BEDFORD, MASSACHUSETTS 01730

AFCRL- 67-0421

Monte Carlo Calculations of Light Scattering From Clouds

Authors

Gilbert N. Plass and George W. Kattawar

Southwest Center for Advanced Studies
Dallas, Texas

Contract No. AF19(628)-5039

Project No. 4076

Task No. 407604

Scientific Report No. 2

23 May 1967

This research was partially supported by the National Aeronautics and Space Administration

Contract Monitor
Robert W. Fenn
Optical Physics Laboratory

Prepared
for

AIR FORCE CAMBRIDGE RESEARCH LABORATORIES
OFFICE OF AEROSPACE RESEARCH
UNITED STATES AIR FORCE
BEDFORD, MASSACHUSETTS 01730

MONTE CARLO CALCULATIONS OF LIGHT SCATTERING FROM CLOUDS

Gilbert N. Plass and George W. Kattawar

Abstract

The scattering of visible light by clouds is calculated from an efficient Monte Carlo code which follows the multiply scattered path of the photon. The single scattering phase function is obtained from the Mie theory by integration over a particle size distribution. The photons are followed through a sufficient number of collisions and reflections from the lower surface (which may have any desired albedo) until they make a negligible contribution to the intensity. Various variance reduction techniques were used to improve the statistics. The reflected and transmitted intensity is studied as a function of solar zenith angle, optical thickness, and surface albedo. The downward flux, cloud albedo, and mean optical path of the transmitted and reflected photons are given as a function of these same parameters. The numerous small angle scatterings of the photon in the direction of the incident beam are followed accurately and produce a greater penetration into the cloud than is obtained with a more isotropic and less realistic phase function.

Gilbert N. Plass is with the Southwest Center for Advanced Studies, P. O. Box 30365, Dallas, Texas 75230.

George W. Kattawar is with North Texas State University, Denton, Texas, 76203 and the Southwest Center for Advanced Studies, P. O. Box 30365, Dallas, Texas 75230.

INTRODUCTION

The multiple scattering of a photon must be taken into account in any study of light reflection and transmission from a cloud. Despite the elegant technique developed by Chandrasekhar [1960] and many others, it is extremely difficult to obtain numerical answers when the single scattering phase function is strongly anisotropic and when the properties of the atmosphere change appreciably with height. Fritz [1954, 1955] and Twomey et al [1967] have obtained interesting results pertaining to clouds, but their results are limited to larger optical depths and directions which are not close to the incident direction by the approximations inherent in their methods.

The present study of light scattering by clouds was made with the Monte Carlo technique which has now become practical with modern high speed digital computers. This method has already been applied to many diverse physical and mathematical problems [Hammersley and Handscomb, 1964]. It has been used by Collins and Wells [1965] in a study of light scattering by atmospheric aerosols.

After a description of our method of calculation, the reflected and transmitted light from a cloud is discussed as a function of optical thickness, surface albedo, and solar incident angle. The albedo of the cloud is presented as a function of surface albedo, optical thickness of the cloud, and incident angle. The downward flux at the lower surface of the cloud and the mean optical path of both the reflected and transmitted photons is discussed.

A Lambert reflecting surface and a single distribution of sizes for the Mie particles is assumed in all these calculations in order to study the dependence on other variables. The cloud is assumed to be horizontally stratified and to be composed of water droplets. Effects due to incident sky radiation, and molecular scattering and absorption are not considered here. The numerous small angle scatterings of the photon in the direction of the incident beam are followed accurately in three dimensions in the present calculation. Among the interesting results is a much greater penetration of the beam into the cloud than is obtained with a more isotropic and less realistic phase function.

MONTE CARLO METHOD

The Monte Carlo method can be applied to any problem if one knows the probability for each step in a sequence of events and desires the probability of the total of all possible events. Thus the Monte Carlo method may be used to study problems in radiative transfer [Collins and Wells, 1965]. However, some of the methods employed in this work differ considerably from theirs.

The advantages of the Monte Carlo method for the study of radiative tranfer in planetary atmospheres are as follows:

1) The calculations may be performed for any single scattering phase function regardless of the degree of anisotropy. The volume averaged phase function may be extremely anisotropic for aerosols and water droplets in the atmosphere. It is virtually hopeless to use conventional methods relying on the expansion of the phase function into a series of Legendre polynomials [Churchill et al, 1966; Coulson et al, 1965].

2) Any relevant parameter such as the single scattering albedo, number density of molecular and aerosol scattering centers, and the various cross-sections may vary with optical depth in the atmosphere.

3) The radiation reflected from a planetary surface may follow any desired distribution, instead of being uniform in angle as required by a Lambert surface. The light reflected from many real surfaces varies greatly with both incident and reflected angle [Coulson et al, 1965].

4) A single computer run will produce fluxes and intensities for both a large number of surface albedos and of detectors in the atmosphere.

5) Any reasonable number of polar and azimuthal angles may be selected.

6) The average mean optical path of both the reflected and transmitted photon may easily be calculated.

The disadvantage of the Monte Carlo method is the fact that the standard deviations of the results are roughly inversely proportional to the square root of the computing times. Therefore the method may not be practical when high accuracy is required.

In our Monte Carlo code the three dimensional path of the photon is followed through a cloud and the atmosphere as it is multiply scattered. The single scattering phase function is obtained by integration of the Mie scattering function over the particle size distribution. The flux and the intensity are calculated for a number of detectors through the atmosphere for a number of surface albedos. In the present calculations the lower surface is assumed to reflect according to Lambert's law.

Several variance reduction techniques minimized the computer time. These included the use of a statistical weight for the photon and a requirement for forced collisions within the atmosphere. A new method was used which takes account of all orders in the reflection from a Lambert's surface with no noticable increase in the computing time. All calculations were performed on an IBM 360-50 computer. The random number generator was the multiplicative congruential generator supplied with the scientific subroutine package. When using this generator to choose a scattering angle from the cumulative distribution function for Mie scattering, it was found necessary to tabulate the function at very small intervals near the strong forward scattering maximum. A linear interpolation was used between the tabulated values.

Every rejection technique used in the program was tested separately. However, the only true test of a Monte Carlo program is in the results of the complete program itself. The reason is that a random number generator may have successive random numbers that have the right properties, but not have a proper distribution of n tuples. Thus our results were tested in a number of cases against known results for isotropic and Rayleigh scattering.

The Monte Carlo results are shown in Figure 1 together with the theoretical results of Chandrasekhar [1960] for isotropic scattering from a semi-infinite atmosphere when the cosine of the incident angle $\mu_o = -0.2$ and the single scattering albedo $\omega_o = 0.2$. All intensities in this paper are normalized to an incident intensity of unity and not to the value π as is sometimes done. All fluxes in this paper are normalized to unit incident flux.

The Monte Carlo results for a Rayleigh phase function are compared in Figure 2 with the exact solution obtained from a program written by Mr. C. N. Adams which employs invariant imbedding techniques. In this example τ (the optical depth) = 1 and curves are shown for the reflected and transmitted intensities for A (surface albedo) = 0 and A = 0.8. The agreement in all cases tested appears very satisfactory.

INTENSITY REFLECTED FROM CLOUDS

The size distribution for the water drops in a cumulus cloud chosen for this calculation is

$$n(r) = 2.373\, r^6 \exp(-1.5r) \quad , \qquad (1)$$

where the radius r is expressed in microns and the concentration n is expressed in $cm^{-3}\mu^{-1}$. This is the distribution function used by Deirmendjian [1964]. We assume a wavelength of 0.7μ for the incident light and a real index of refraction of 1.33 for the water drops. The results are also applicable to other visible wavelengths if the size of the particles is adjusted in proportion to the wavelength.

The angular intensity function for single scattering is calculated from our Mie program which is described elsewhere [Kattawar and Plass, 1967]. The results are averaged over the size distribution of the drops and over the two directions of polarization. The resulting intensity function is shown in Figure 3. There is an exceedingly sharp forward-scattering maximum which is shown in more detail in the inset in the upper left corner.

From this function a cumulative probability distribution was calculated. It was necessary to specify this curve at over 240 points with variable spacing in order to be certain that the particles are scattered according to the details of this curve. A linear interpolation technique was used between tabulated points.

The reflected and transmitted intensities for a cloud with the size distribution given by Eq. (1) is shown in Figures 4 and 5. The sunlight is incident vertically so that μ_o (cosine of incident zenith angle) = -1.0. Curves are given for clouds with an optical depth τ from 0.01 to 30. The intensity is shown in each case when the surface albedo A = 0 and when A = 1. The transmitted intensity does not include the incident photon until it has been scattered for the first time.

When a cloud is sufficiently thin, the scattered intensity approaches the value which would be calculated from single scattering events only. The intensity calculated from the phase function shown in Figure 3 for single scattering only is indicated in Figures 4 and 5 by small squares when τ = 0.01 and 0.1 and when A = 0. In general there is excellent agreement between these results and those of the Monte Carlo calculation. This provides another check on the Monte Carlo method. Most of the variation in the intensity curve as a function of μ is due to the nature of the phase function and is not caused by fluctuations in the result.

The single scattering value is too high for both the reflected and transmitted beam for the range $0.0 \leq \mu \leq 0.1$ and τ = 0.1. This means that the cloud is already sufficiently thick close to the horizontal direction when τ = 0.1 so that multiple scattering must be taken into account.

For the range $0.9 \leq \mu \leq 1.0$, the single scattering values of the transmitted intensity are too low for both $\tau = 0.1$ and 0.01. The actual intensity is much larger because of the many small angle scattering events which occur with this phase function. The deviations of the multiply-scattered intensities from the single scattering values for $0.1 \leq \mu \leq 0.9$ provides an indication of the statistical fluctuation in our Monte Carlo results. The statistical fluctuation is expected to be larger when the intensities are small (as they are for $\tau = 0.01$) rather than when they are closer to unity.

When the surface albedo $A = 0$, the reflected intensity as shown by Fig. 4 is a maximum near the horizon for clouds whose optical thickness τ is small. The intensity decreases as μ^{-1} away from the horizon as the number of single scattering centers decreases along the line of sight. The maximum in the curve near $\mu = 0.7$ for small τ is due to the maximum in the angular intensity function near $\mu = -0.75$ as shown in Figure 3. When $\tau = 1$, the reflected intensity is more nearly uniform at all angles because of multiple scattering effects. For large τ, the reflected intensity has a minimum at the horizon and a maximum at the zenith.

When $A = 1$, the reflected intensities are much more nearly the same at all angles. The intensity is essentially uniform over angle for small τ, since the uniformly reflected radiation from the Lambert surface is not appreciably modified by the cloud. For clouds with large τ, the reflected intensity is a minimum near the horizon since the radiation reflected from the planetary surface can not penetrate the cloud at these large zenith angles.

The transmitted intensity in Figure 5 has a large maximum near the zenith for thin clouds because of the large number of small angle scatterings around the original direction of the beam. This maximum persists even up to $\tau = 30$ for $A = 0$, although it is very much less pronounced. There is another maximum in the curves for thin clouds near the horizon because of the cosine effect. However, this changes to a minimum for thick clouds.

The transmitted intensity as shown in Figure 5 is appreciably larger near the horizon at all τ for $A = 1$ than for $A = 0$. The reason is that the radiation reflected from the Lambert's surface near the horizon has a much greater chance of being reflected back to this surface if it makes one or more small angle collisions (see Figure 3). In this case it makes a contribution to the intensity near the horizon. In order to contribute to the downward intensity at an angle close to the zenith, the photon must undergo large angle scattering which is much less probable.

When $\mu_o = 1.0$, the intensities are azimuth independent. This is not the case for other angles of incidence. We can use as many intervals as desired for both the zenith and azimuthal angles in our Monte Carlo program within certain restrictions on memory size. It was decided to use only two intervals for the azimuthal angle for other angles of incidence for ease of presentation of the results. The results for $\mu_o = -0.5$ are shown in Figs. 6-9. Take $\phi = 0°$ at the intersection of the horizontal plane and the plane containing the incident beam and in the direction of the incident beam. Then the ϕ intervals used in this calculation are: (1) $-90° \leq \phi \leq 90°$; (2) $90° \leq \phi \leq 270°$. The results for interval (1) are shown on the left hand side of Figures 6-9 and

those for interval (2) on the right hand side, i.e. one intensity curve shows the variation from one horizon to the zenith back to the other horizon averaged in each case over the ϕ angles indicated above.

The reflected intensity for thin clouds shown in Figure 6 for A = 0 is largest near the horizon nearest the direction of the incident beam. It falls off very regularly to a minimum near the zenith and then rises less rapidly to a smaller value on the opposite horizon. The value at the minimum is 500 times smaller than at the maximum. This curve results both from the cosine term near the horizon and the greatly reduced probability for backscattering compared to forward scattering. As the optical depth of the cloud increases, the intensity curves follow qualitatively the same variation, but the magnitude of the variations is greatly reduced by multiple scattering.

The intensity when A = 1 again has relatively little dependence on angle as is shown in Figure 7. The intensity is nearly constant for thin clouds. For thick clouds it has a small maximum near the point on the horizon closest to the direction of the original beam and a minimum at the opposite horizon.

When A = 0 the transmitted intensity as shown in Figure 8 has a maximum in the direction of the original beam for $\tau \leq 3$. This is expected from the numerous multiple small angle scattering events around the original direction. The minimum transmitted intensity is near $\mu = 0.8$ on the opposite side from the direction of the original beam. This is caused by the single scattering probability decreasing rapidly as the angle increases in this range. For thick clouds the intensity is relatively constant,

but shows a tendency to be two to three times smaller near the horizon than at the zenith.

When A = 1, the qualitative shape of the curves shown in Figure 9 is the same as in Figure 8. The values are larger near the horizons as the albedo increases due to the photons reflected from the Lambert surface into an angle near the horizon and then back-scattered into a downward direction near the horizon by the many probable small angle scatterings. The curves for large τ are very uniform.

Similar curves for sunlight incident near the horizontal at $\mu_o = -0.1$ are given in Figures 10-13. The reflected intensity shown in Figure 10 is similar to the curves for $\mu_o = -0.5$ except that the variations in the curves are greater and all curves show a pronounced minimum near the zenith. Even a thick cloud reflects ten times as much light toward the horizon in the direction of the incident beam as it does to the zenith. The photons can escape from the cloud easily in this direction by many probable small angle scatterings.

The reflected intensity when A = 1 also shows more variation than before as shown in Figure 11. All curves have a maximum at the near horizon and a minimum near the zenith.

The transmitted intensity as shown in Figure 12 for the case A = 0 shows the expected maximum for thin clouds around the direction of the original beam. For thin clouds the maximum transmitted intensity at the horizon is 6000 times larger than the minimum value near the zenith. When A = 1, Figure 13 shows again that the effect of reflected photons from the planetary surface is predominately to increase the transmitted

intensity near the horizon. It is interesting to note in most cases when $\tau \leq 1$ that there is a considerable region in which the transmitted intensity is nearly proportional to exp [-(const)μ]. When τ is large the intensity is several times larger at the zenith than at the horizon.

The variation of the reflected and transmitted intensities with solar angle is further illustrated by Figures 14 and 15 for $\mu_o = -0.02$. When the incident beam is so close to the horizon, the reflected intensity has a very strong maximum at the forward horizon even for thick clouds. When $\tau = 10$, the intensity near the horizon is more than 100 times greater than that at the zenith and 20 times greater than the intensity at the far horizon. The shapes of the transmitted intensity curves are rather similar for $\mu_o = -0.02$ and $\mu_o = -0.1$. However, the transmitted intensity is smaller in the former case because of the larger cloud albedo.

Some of the results of Twomey et al [1967] may be compared with these curves. This method is only valid for $\tau > 1$ and does not take account of the numerous small angle scatterings accurately as is done in our calculation. Our curves show in general stronger maxima around the direction of the original beam and differ numerically from some of his results.

FLUX

The downward diffuse flux at the lower boundary of the cloud as a function of optical thickness is shown in Figure 16 for A = 0. A photon is not counted in the diffuse flux until it has undergone one scattering event. All fluxes are normalized to unit incident flux. The flux is small for small τ, since there are not enough water droplets to scatter

an appreciable number of photons. The flux increases with τ until the curves reach a maximum. The intensity decreases rapidly with further increases in τ, since the cloud is so thick that the photons have a greater probability of escaping from the upper surface than in finding their way to the bottom. The maximum flux occurs at successively smaller values as the incident beam approachs the horizon.

When the surface albedo is high, the downward flux at the lower surface of the cloud under certain conditions may be greater than the incident flux, as was first pointed out by Fritz [1955]. The downward flux (including the contribution from the unscattered incident flux normalized to unity at the cloud top) is shown in Figure 17 as a function of optical thickness for four different values of μ_o when A = 1. When μ_o = -1.0 and τ = 6, the downward flux is 22% greater than the incident flux. When μ_o = -0.5, the downward flux is 0.13% greater than the incident flux when τ = 0.1. The downward flux is always less than unity for μ_o near the horizon. The large effect when the incident beam is vertical is connected with the strong forward scattering of the particles. A relatively large fraction of the radiation is transmitted through the cloud near the vertical, but finds it difficult to escape back out because the photons are now traveling in almost random directions. When μ_o = -1.0 and τ = 0, the downward flux is greater than unity for all A > 0.4. For example, the downward flux is 1.0994 when A = 1; 1.0662 when A = 0.8; 1.0350 when A = 0.6; 0.9937 when A = 0.4; 0.9514 when A = 0.

The strong penetration of radiation into a cloud composed of water droplets larger than the wavelength is shown by a comparison of the flux calculated here with that for Rayleigh scattering. For example, when $\mu_o = -1.0$ and A = 1 the downward flux is 0.6573 for Rayleigh scattering, but 1.0994 for Mie scattering. The difference is even larger between the diffuse intensity in the zenith direction which is 0.0977 for Rayleigh scattering and 0.648 for Mie scattering.

MEAN OPTICAL PATH

The mean optical path of the photon is a quantity of interest in several types of problems. For example, when the reflected light from clouds is measured from a satellite, a knowledge of the mean optical path is necessary to allow for molecular absorption at certain wavelengths.

The mean optical path of the reflected photon is shown in Figure 18 for various angles of incidence. For thin clouds of a given optical thickness, the mean optical path is greater the closer the incident beam is to the horizon. The photon in this case travels a greater distance along the beam direction before being scattered back out.
For thick clouds of a given optical thickness, the mean optical path is greatest for an incident beam at the zenith. In this case the photon on the average penetrates deeply into the cloud. Because of the single scattering phase function, the photon is more likely to be scattered in an upward direction by a single collision when the incident beam is nearly horizontal. For example, when the cloud's optical thickness $\tau = 10$, the mean optical path for the reflected photon is 24.2 for $\mu_o = -1.0$; 20.8 for $\mu_o = -0.5$; 12.9 for $\mu_o = -0.1$; 9.47 for $\mu_o = -0.02$.

The curves cross over one another in the region from $\tau = 1$ to 10.

The mean optical path of the transmitted photon is shown in Figure 19. This quantity for a given cloud thickness always increases as the incident beam moves from the zenith to the horizon. The differences for various incident angles are large for thin clouds and very small for thick clouds. When $\mu_o = -1.0$, the photon efficiently penetrates the cloud as it undergoes many small angle forward scatterings. When $\mu_o = -0.02$, the photon on the average travels a distance of the order $\tau = 1$ before it undergoes a large angle scattering collision. After one large angle collision the photon essentially loses its memory of its initial direction. Thus all photons travel approximately the same distance from this point until they leave the lower surface of the cloud. This is the reason all the mean optical paths are nearly the same for large τ. For example, when $\tau = 10$, the mean optical thickness of the transmitted photon is 19.2 for $\mu_o = -1.0$; 24.9 for $\mu_o = -0.5$; 28.0 for $\mu_o = -0.1$, 28.2 for $\mu_o = -0.02$.

Mean optical paths for $\tau > 2$ and $\mu_o = -0.55$ have been given by Twomey et al [1967]. The curves are qualitatively similar to those shown here. Our reflected mean optical paths are larger than theirs. This is presumably because our calculations accurately allows for the numerous small angle scatterings which allow the photon to penetrate deeper into the cloud and thus to have a greater optical path. It may also be due to the fact that their single scattering phase function is somewhat different from ours.

CLOUD ALBEDO

The cloud albedo is defined as the fraction of the incident light reflected from the cloud. It is shown in Figures 20-24 for various angles of incidence μ_o and surface albedos A.

The cloud albedo for $\mu_o = -1.0$ is shown in Figure 20. When the planetary surface is completely absorbing (A = 0), the cloud does not reflect appreciable radiation until τ is of the order of unity. The cloud albedo then rises rapidly until it is 0.88 when $\tau = 100$. When A = 1, the cloud albedo has the value unity for all τ, since no absorption was assumed by the water droplets in this calculation.

For A = 0.8, the cloud albedo is 0.8 when the cloud is sufficiently thin. As τ increases, the albedo first decreases since the increased reflection by the cloud is more than offset by the increased downward scattering of the radiation reflected form the planetary surface. The minimum cloud albedo in this case is 0.782 near $\tau = 3$. A similar minimum also occurs for A = 0.4 and 0.6. The cloud albedo rises as τ increases beyond this point.

The cloud albedos for $\mu_o = -0.5$, -0.1, and -0.02 are shown in Figures 21-23. These curves have the same shape as that for $\mu_o = -1.0$, except that there is no longer a small minimum in the curves for A = 0.4 to 0.8. Because of the strong forward scattering, the cloud albedo always increases with τ when $|\mu_o| \leq 0.5$.

The cloud albedo also always increases as $|\mu_o|$ decreases for a fixed τ and A. For example, when $\tau = 0.1$ and A = 0, the cloud albedo is 0.00468 when $\mu_o = -1.0$; 0.0181 when $\mu_o = -0.5$, 0.180 when $\mu_o = -0.1$;

0.492 when μ_o = -0.02. When τ = 10 and A = 0, the cloud albedo increases from 0.466 when μ_o = -1.0 to 0.852 when μ_o = -0.02.

The cloud albedos shown here are appreciably smaller than those given by Fritz [1954] in his Figure 4. This is probably explained by the penetration to a greater depth by the actual photons through multiple small angle scattering as described in our calculation. Our values are also usually less than those of Korb and Möller [1962] presumably for the same reason.

The curves of cloud albedo for various values of A approach each other more closely as τ increases. This merely states that a relatively smaller percentage of the photons is able to reach the planetary surface and return to the upper surface as τ becomes large. An important point is that there can be significant variations in the cloud albedo as the surface albedo changes for values of τ between 10 and 100, as shown in Figures 20-23. The optical thickness of Venus is usually placed in this range. Table I shows the cloud albedo for τ = 10 and 30, for various values of μ_o and surface albedo A. It is immediately obvious that the reflected flux still depends appreciably on the surface albedo even for large τ. Thus there is the possibility of obtaining information about conditions beneath a thick cloud layer from a study of the reflected light because of the strong penetration in the direction of the original beam allowed by the many small angle scatterings undergone by the photon.

TABLE I. CLOUD ALBEDO

τ	μ_o	A = 0	A = 0.2	A = 0.4	A = 0.6	A = 0.8
10	-1.0	0.466	0.519	0.588	0.679	0.807
10	-0.5	.638	.674	.721	.782	.869
10	-0.1	.799	.819	.845	.880	.928
10	-0.02	.852	.867	.886	.912	.947
30	-1.0	.773	.786	.803	.831	.881
30	-0.5	.818	.827	.840	.861	.901
30	-0.1	.900	.905	.912	.924	.946

REFERENCES

1. Chandrasekhar, S., Radiative Transfer, Dover Publications, New York, New York, 1960.
2. Churchill, S. W., Chu, C. M., Leacock, J. A., and Chen, J. "The Effect of Anisotropic Scattering on Radiative Transfer", The University of Michigan Research Institute, Ann Arbor, Mich. 231 pp, 1966.
3. Collins, D. G. and Wells, M. B. Monte Carlo Codes for the Study of Light Transport in the Atmosphere, Vol's I & II, Radiation Research Associates, Inc., Fort Worth, Texas, 1965.
4. Coulson, K. L., Bouricius, G. M., and Gray, E. L., Optical Reflection Properties of Natural Surfaces, J. Geophys. Res., 70, 4601-4611, 1965.
5. Diermendjian, D., Scattering and Polarizations Properties of Water Clouds and Hazes in the Visible and Infrared, Appl. Opt. 3, 187-196 (1964).
6. Fritz, S.,Scattering of Solar Energy by Clouds of "Large Drops", J. J. Meteorology II, 291-300 (1954).
7. Fritz, S., Illuminance and Luminance under Overcast Skies, J. Opt. Soc. Amer. 10, 820-825 (1955).
8. Kattawar, G. W., and G. N. Plass, Appl. Opt. (in press) (1967).
9. Korb, G., and F. Möller, Theoretical Investigation on Energy Gain by Absorption of Solar Radiation in Clouds, Final Technical Report, 1962, Meteorologisches Institut, Munich, Germany.
10. Twomey, S., H. Jacobowitz, and H. B. Howell, Light Scattering by Cloud Layers, J. Atmospheric Sciences 24, 70-79 (1967).

LEGENDS FOR FIGURES

Fig. 1. Reflected intensity from a semi-infinite atmosphere with isotropic scattering, μ_o (cosine of incident angle) = -0.2, and ω_o (single scattering albedo) = 0.2 as a function of μ (cosine of zenith angle). The continuous curve is calculated from Chandrasekhar [1960]. The Monte Carlo results are for 20,000 histories. The incident intensity is normalized to unity.

Fig. 2. Reflected and transmitted intensity for a Rayleigh phase function for an atmosphere with τ (optical depth) = 1. The upper curves are for A (surface albedo) = 0.8 and the lower curves are for A = 0. The continuous curve was calculated by a program written by Mr. C. N. Adams. The Monte Carlo results are for 30,000 histories.

Fig. 3. Angular intensity function for Mie scattering as a function of the cosine μ of scattering angle averaged over the size distribution given by Eq. (1) and over the two directions of polarization. The inset in upper left shows the curve near $\mu = 1$. It is assumed that the wavelength of the incident light is 0.7μ and that the index of refraction of the water drops is 1.33.

Fig. 4. The reflected intensity is shown as a function of μ, the cosine of the zenith angle. The curves on the left and right portion of the figure are for A (surface albedo) = 0 and 1 respectively. The optical depth of the cloud is τ. The sunlight is incident vertically, μ_o (cosine of incident zenith angle) = -1.0. The incident intensity is normalized to unity.

Fig. 5. Transmitted intensity for μ_o = -1.0 and A = 0 and 1. The transmitted intensity does not include the incident photon until it has been scattered the first time. See caption for Fig. 4.

Fig. 6. Reflected intensity for μ_o = -0.5 and A = 0 as a function of μ, the cosine of the zenith angle. The left hand portion of the graph refers to values averaged over the azimuthal angle for 90° on both sides of the direction of the original beam. The values on the right portion of the graph are for values averaged over the remaining azimuthal angles. Thus one intensity curve from left to right shows the variation from one horizon to the zenith and back to the other horizon averaged over the indicated azimuthal angles.

Fig. 7. Reflected intensity for μ_o = -0.5 and A = 1. See caption for Fig. 6.

Fig. 8. Transmitted intensity for μ_o = -0.5 and A = 0. See caption for Fig. 6.

Fig. 9. Transmitted intensity for μ_o = -0.5 and A = 1. See caption for Fig. 6.

Fig. 10. Reflected intensity for μ_o = -0.1 and A = 0. See caption for Fig. 6.

Fig. 11. Reflected intensity for μ_o = -0.1 and A = 1. See caption for Fig. 6.

Fig. 12. Transmitted intensity for μ_o = -0.1 and A = 0. See caption for Fig. 6.

Fig. 13. Transmitted intensity for μ_o = -0.1 and A = 1. See caption for Fig. 6.

Fig. 14. Reflected intensity for μ_o = -0.02 and A = 0. See caption for Fig. 6.

Fig. 15. Transmitted intensity for $\mu_o = -0.02$ and A = 0. See caption for Fig. 6.

Fig. 16. Downward diffuse flux at lower boundary of cloud as a function of optical thickness for $\mu_o = -1.0, -0.5, -0.1$ and for A = 0. The incident flux is normalized to unity in each case.

Fig. 17. Downward diffuse flux plus remaining flux from incident beam at lower boundary of cloud as a function of optical thickness of cloud for $\mu_o = -1.0, -0.5, -0.1, -0.02$ and for A = 1. The incident flux is normalized to unity in each case.

Fig. 18. Mean optical path of reflected photon as a function of optical thickness of cloud for $\mu_o = -0.02, -0.1, -0.5, -1.0$.

Fig. 19. Mean optical path of transmitted photon as a function of optical thickness of cloud for $\mu_o = -0.02, -0.1, -0.5, -1.0$.

Fig. 20. Cloud albedo as a function of optical thickness for $\mu_o = -1.0$ and A = 0, 0.2, 0.4, 0.6, 0.8.

Fig. 21. Cloud albedo as a function of optical thickness for $\mu_o = -0.5$ and A = 0, 0.2, 0.4, 0.6, 0.8.

Fig. 22. Cloud albedo as a function of optical thickness for $\mu_o = -0.1$ and A = 0, 0.2, 0.4, 0.6, 0.8.

Fig. 23. Cloud albedo as a function of optical thickness for $\mu_o = -0.02$ and A = 0, 0.2, 0.4, 0.6, 0.8.

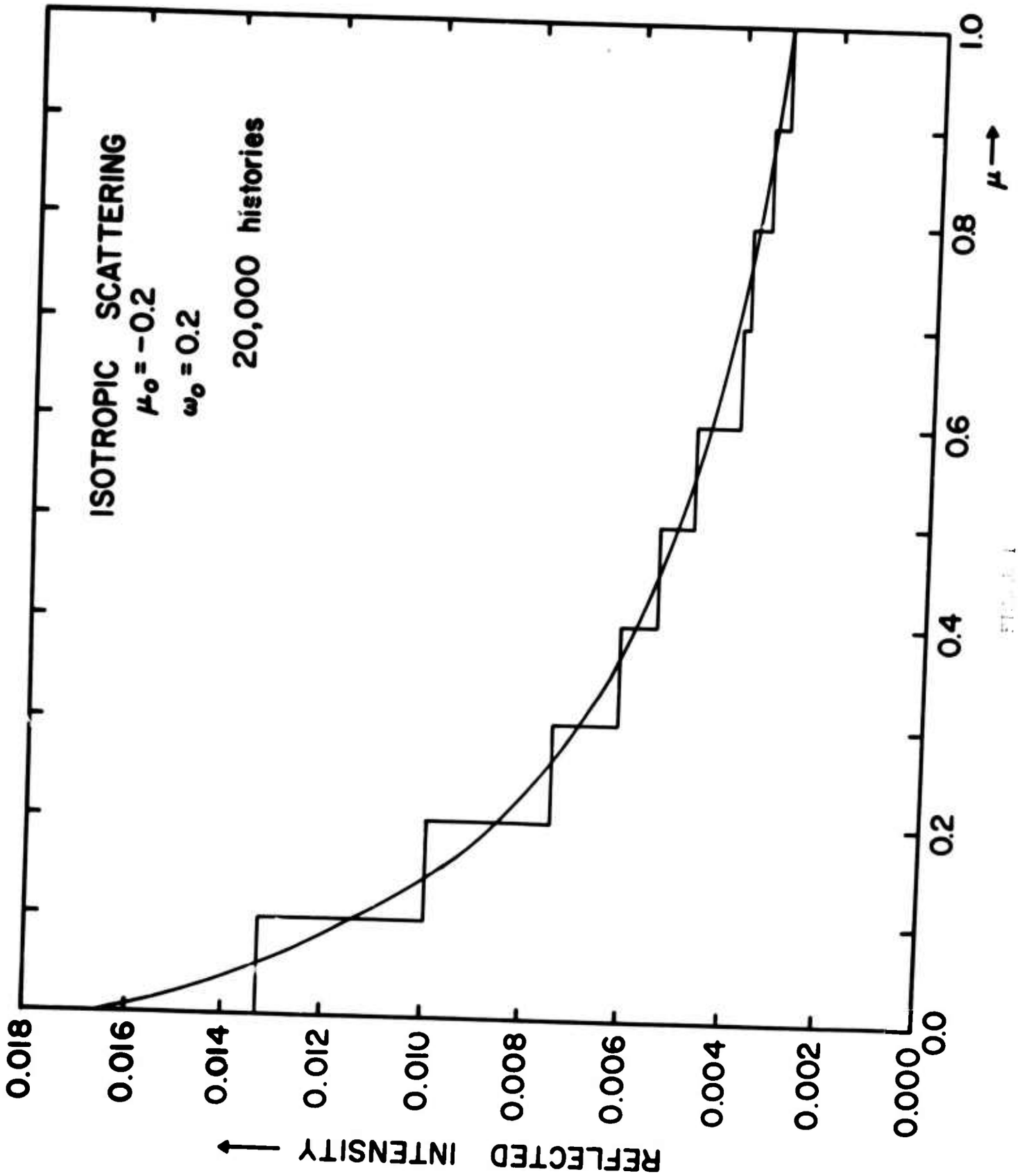
ISOTROPIC SCATTERING
$\mu_0 = -0.2$
$\omega_0 = 0.2$
20,000 histories
REFLECTED INTENSITY ⟵
μ ⟶
0.000
0.002
0.004
0.006
0.008
0.010
0.012
0.014
0.016
0.018
0.0
0.2
0.4
0.6
0.8
1.0

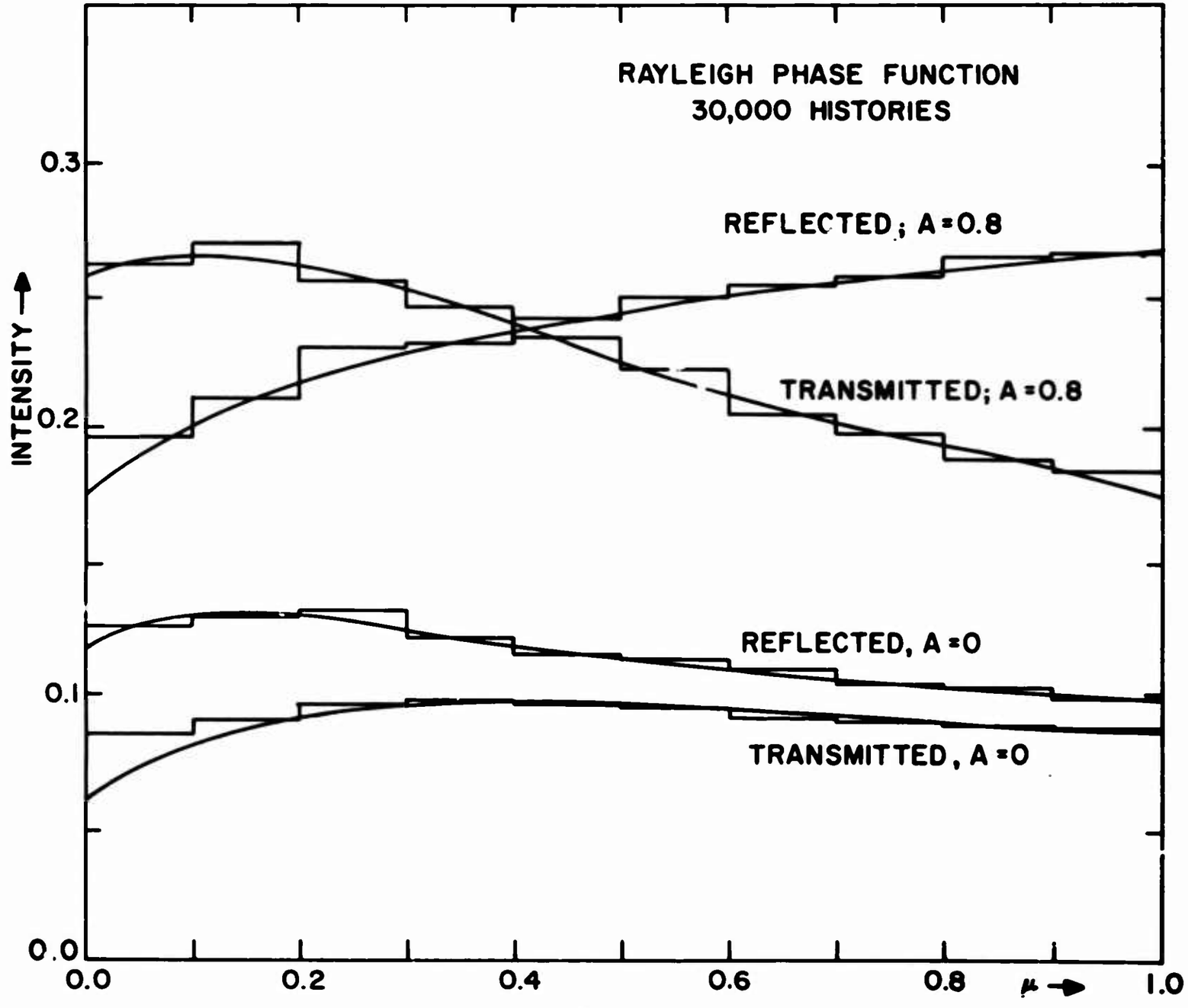
RAYLEIGH PHASE FUNCTION
30,000 HISTORIES
REFLECTED; A=0.8
TRANSMITTED; A=0.8
REFLECTED, A=0
TRANSMITTED, A=0
INTENSITY
0.0
0.1
0.2
0.3
0.0
0.2
0.4
0.6
0.8
1.0
μ

FIGURE 2

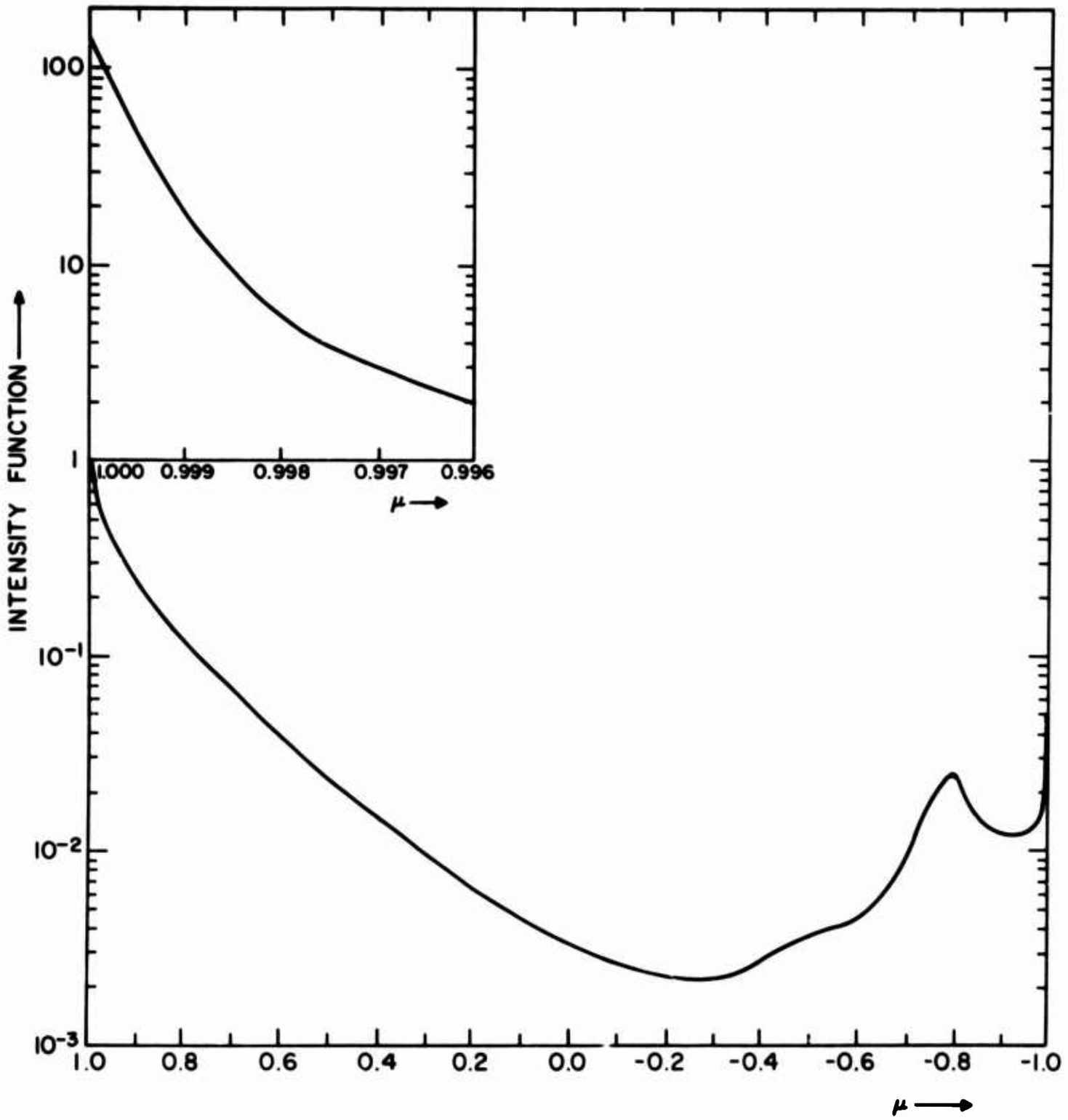
INTENSITY FUNCTION
100
10
1
10^{-1}
10^{-2}
10^{-3}
1.000
0.999
0.998
0.997
0.996
μ
1.0
0.8
0.6
0.4
0.2
0.0
-0.2
-0.4
-0.6
-0.8
-1.0
μ

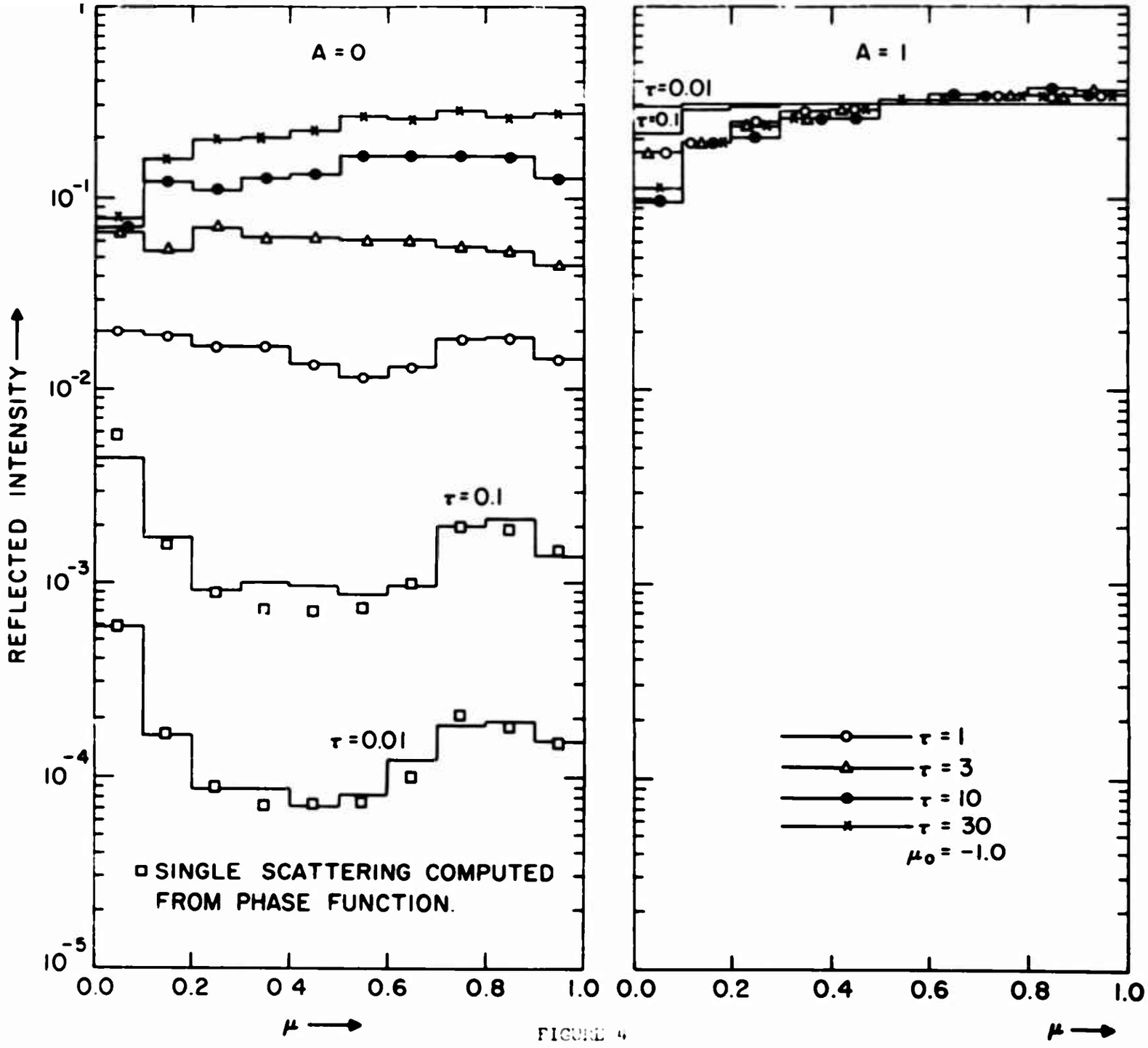
A = 0
A = 1
REFLECTED INTENSITY
τ=0.01
τ=0.1
τ = 1
τ = 3
τ = 10
τ = 30
μ₀ = -1.0
□ SINGLE SCATTERING COMPUTED FROM PHASE FUNCTION.
μ
0.0
0.2
0.4
0.6
0.8
1.0

FIGURE 4

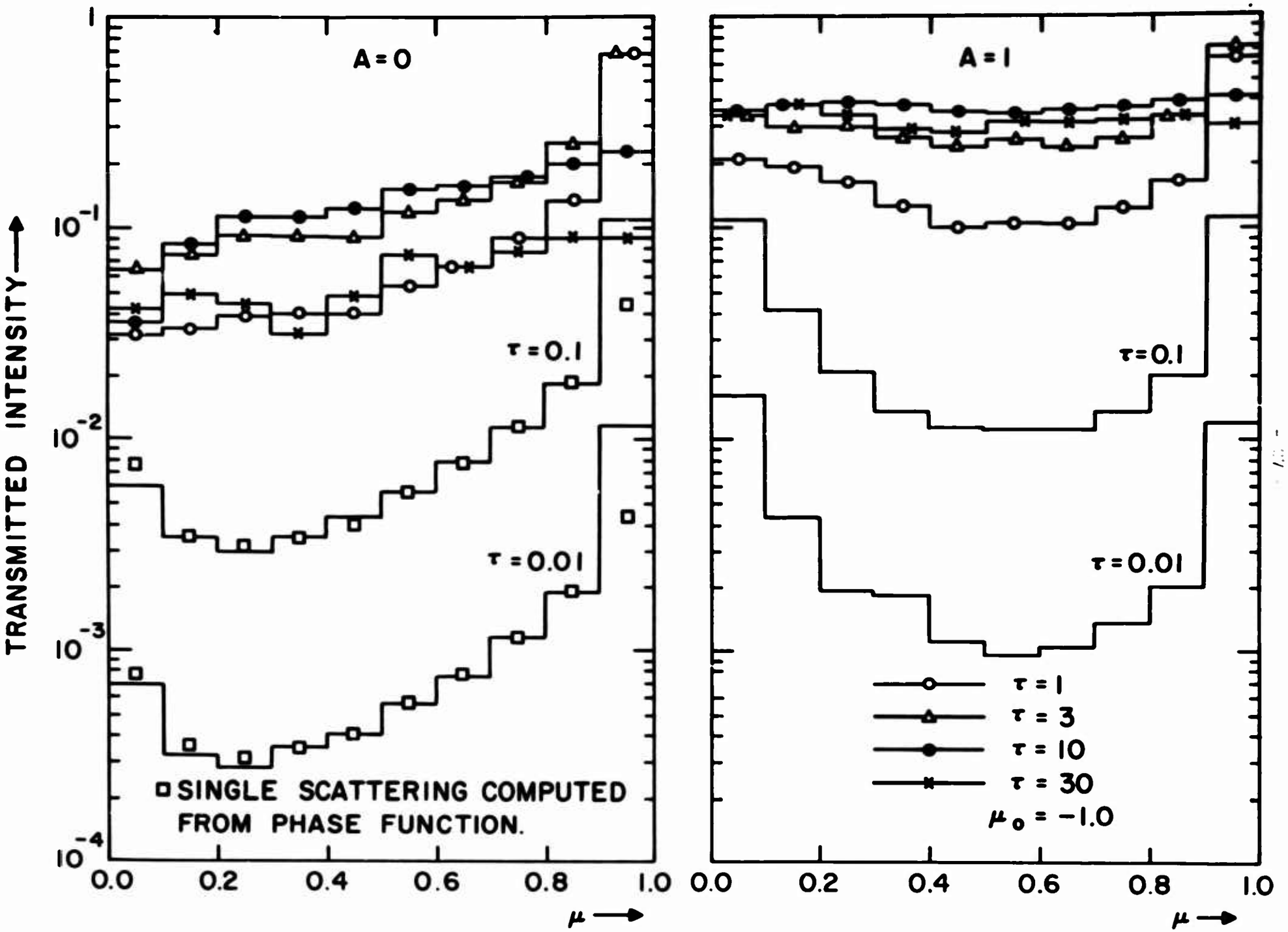
A=0
A=1
TRANSMITTED INTENSITY
1
10^{-1}
10^{-2}
10^{-3}
10^{-4}
τ = 0.1
τ = 0.01
SINGLE SCATTERING COMPUTED FROM PHASE FUNCTION.
τ = 1
τ = 3
τ = 10
τ = 30
$\mu_0 = -1.0$
0.0
0.2
0.4
0.6
0.8
1.0
μ

FIGURE 5

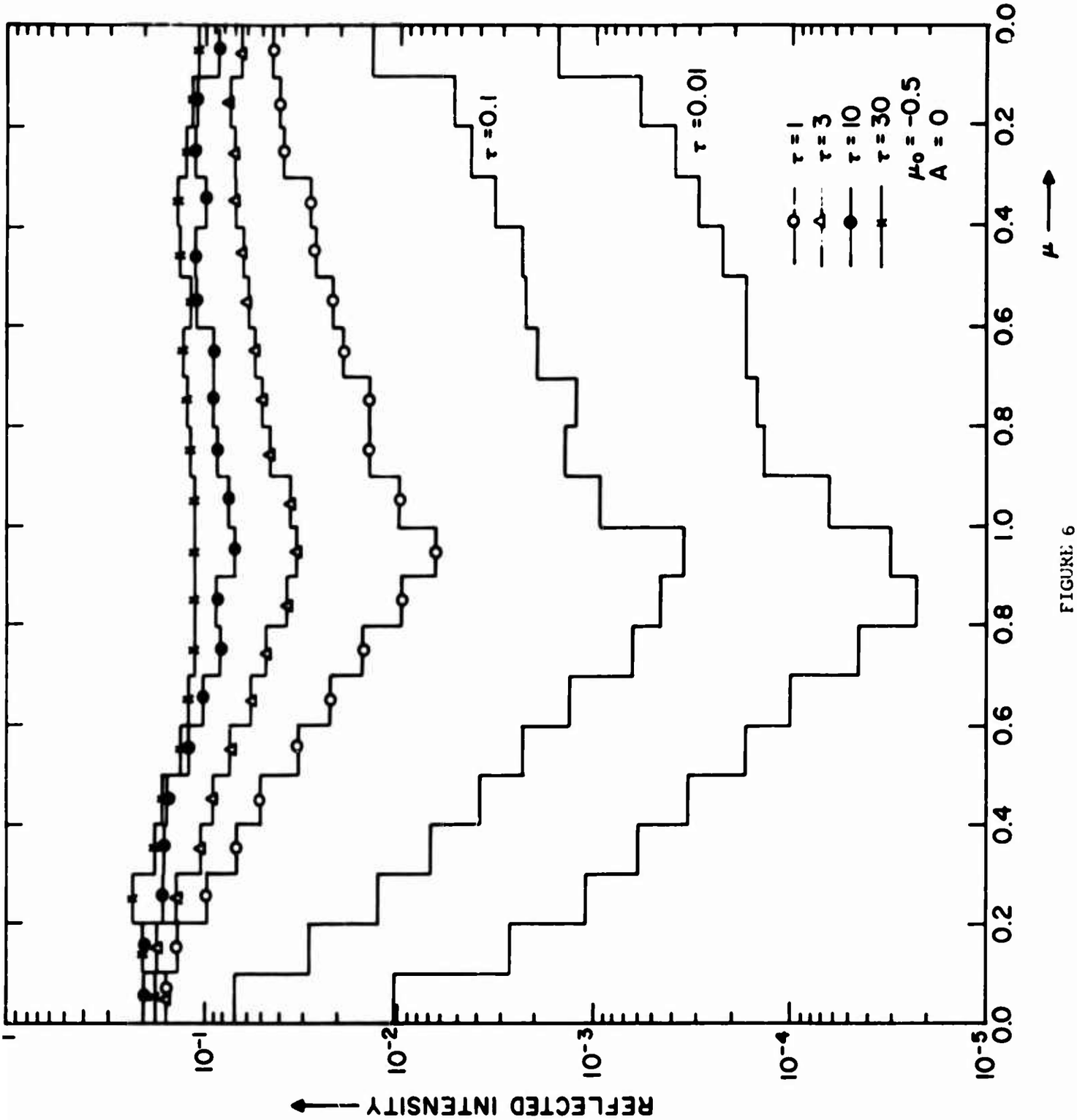
REFLECTED INTENSITY
10^{-1}
10^{-2}
10^{-3}
10^{-4}
10^{-5}
0.0
0.2
0.4
0.6
0.8
1.0
0.8
0.6
0.4
0.2
0.0
μ
τ =0.1
τ =0.01
τ = 1
τ = 3
τ = 10
τ = 30
$\mu_0 = -0.5$
A = 0

FIGURE 6

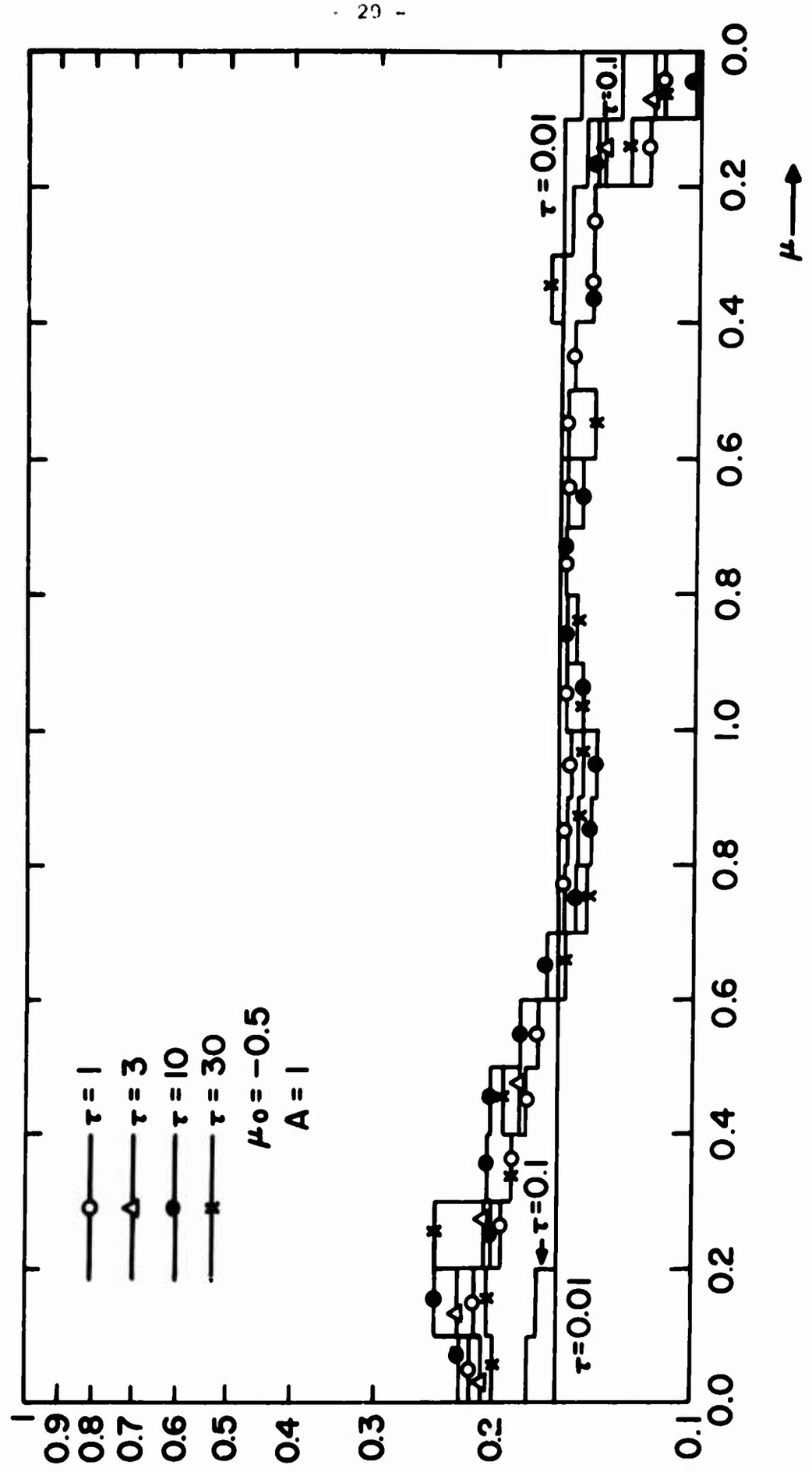
REFLECTED INTENSITY
1
0.9
0.8
0.7
0.6
0.5
0.4
0.3
0.2
0.1
0.0
0.2
0.4
0.6
0.8
1.0
0.8
0.6
0.4
0.2
0.0
μ
τ = 1
τ = 3
τ = 10
τ = 30
μ₀ = −0.5
A = 1
τ=0.01
τ=0.1
τ=0.01
τ=0.1

FIGURE 7

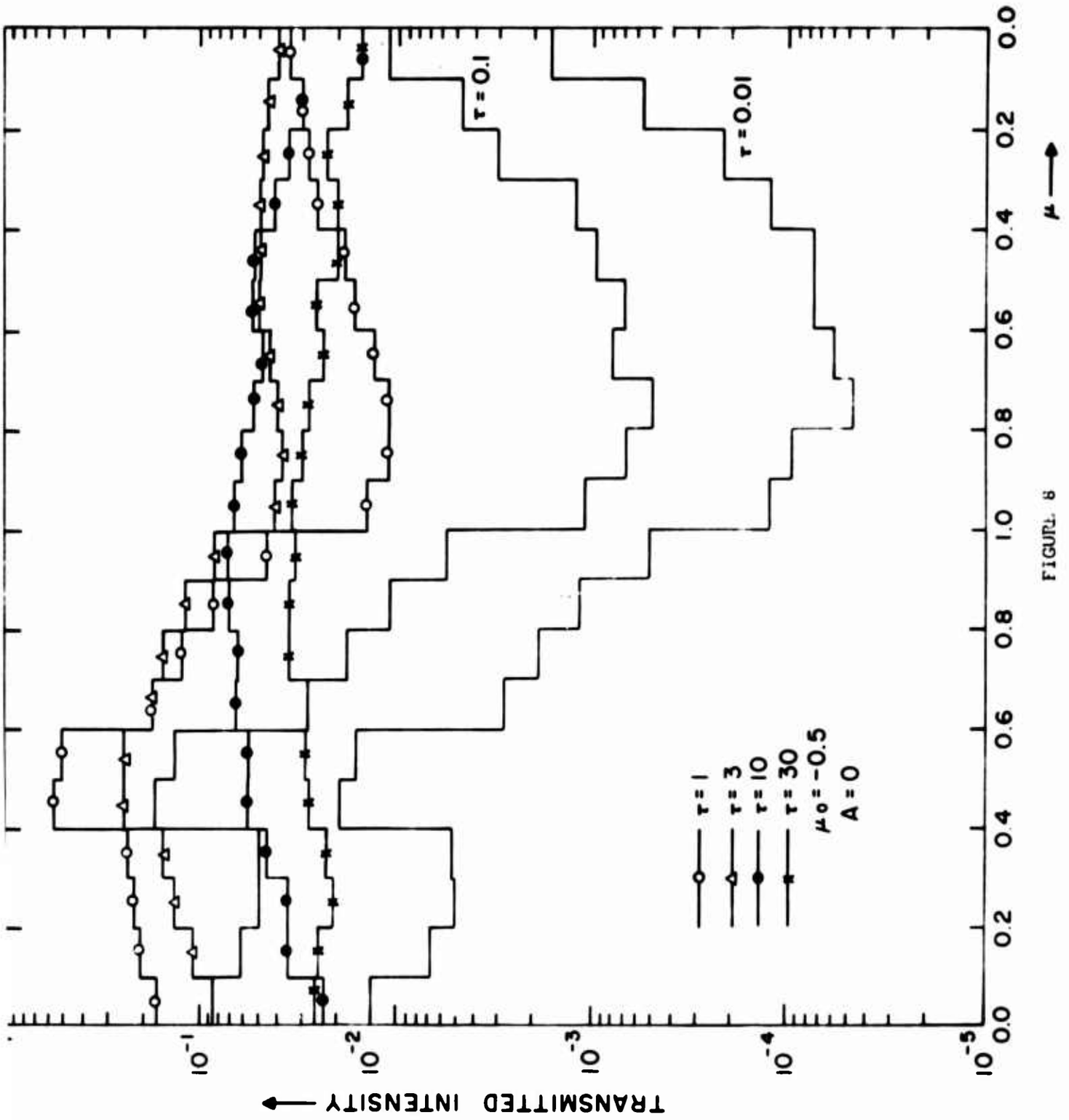
TRANSMITTED INTENSITY
10^{-1}
10^{-2}
10^{-3}
10^{-4}
10^{-5}
0.0
0.2
0.4
0.6
0.8
1.0
0.8
0.6
0.4
0.2
0.0
μ
τ = 0.1
τ = 0.01
τ = 1
τ = 3
τ = 10
τ = 30
μ₀ = -0.5
A = 0

FIGURE 8

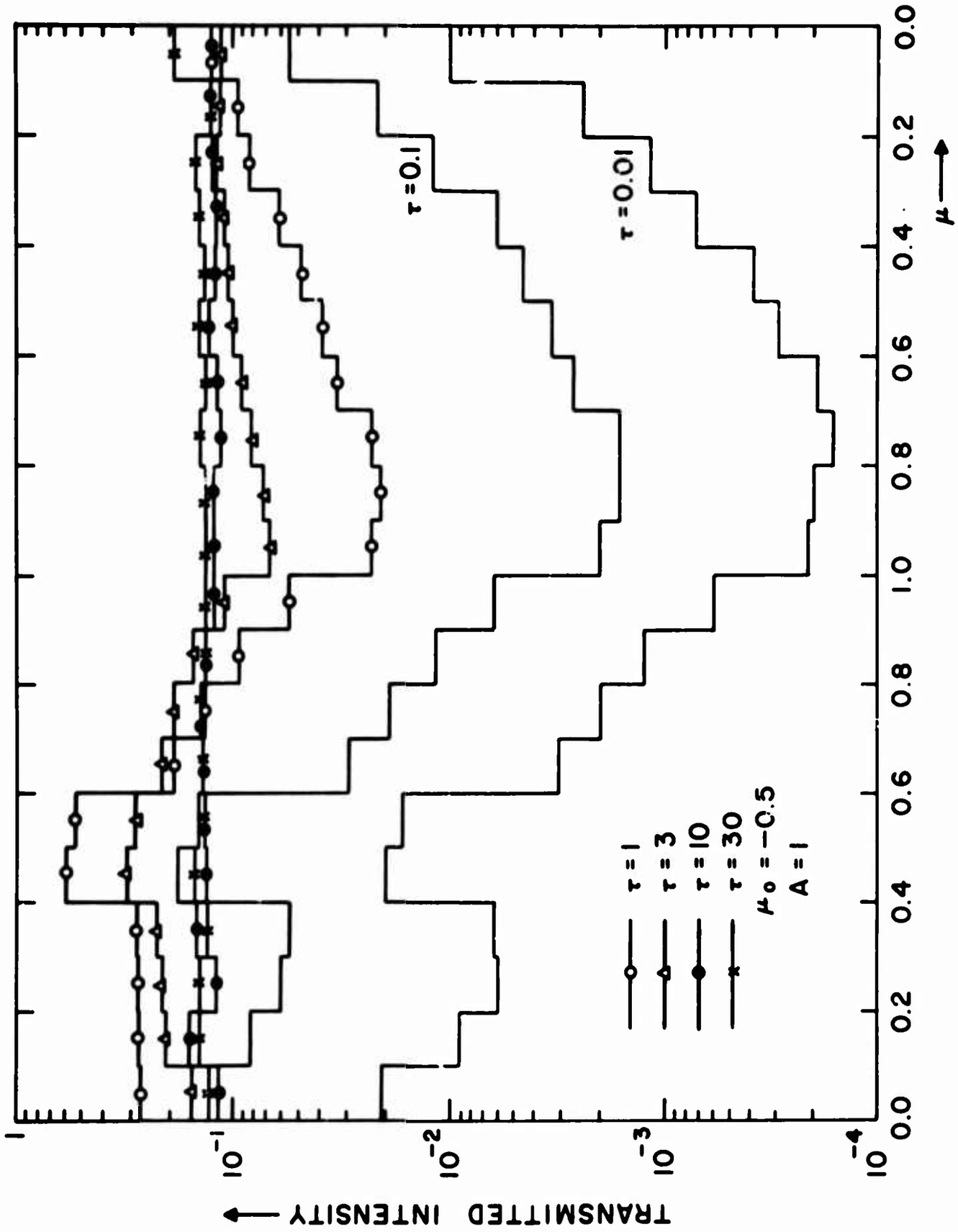
TRANSMITTED INTENSITY
10^{-1}
10^{-2}
10^{-3}
10^{-4}
0.0
0.2
0.4
0.6
0.8
1.0
0.8
0.6
0.4
0.2
0.0
μ
τ=0.1
τ=0.01
τ = 1
τ = 3
τ = 10
τ = 30
$\mu_o = -0.5$
A = 1

FIGURE

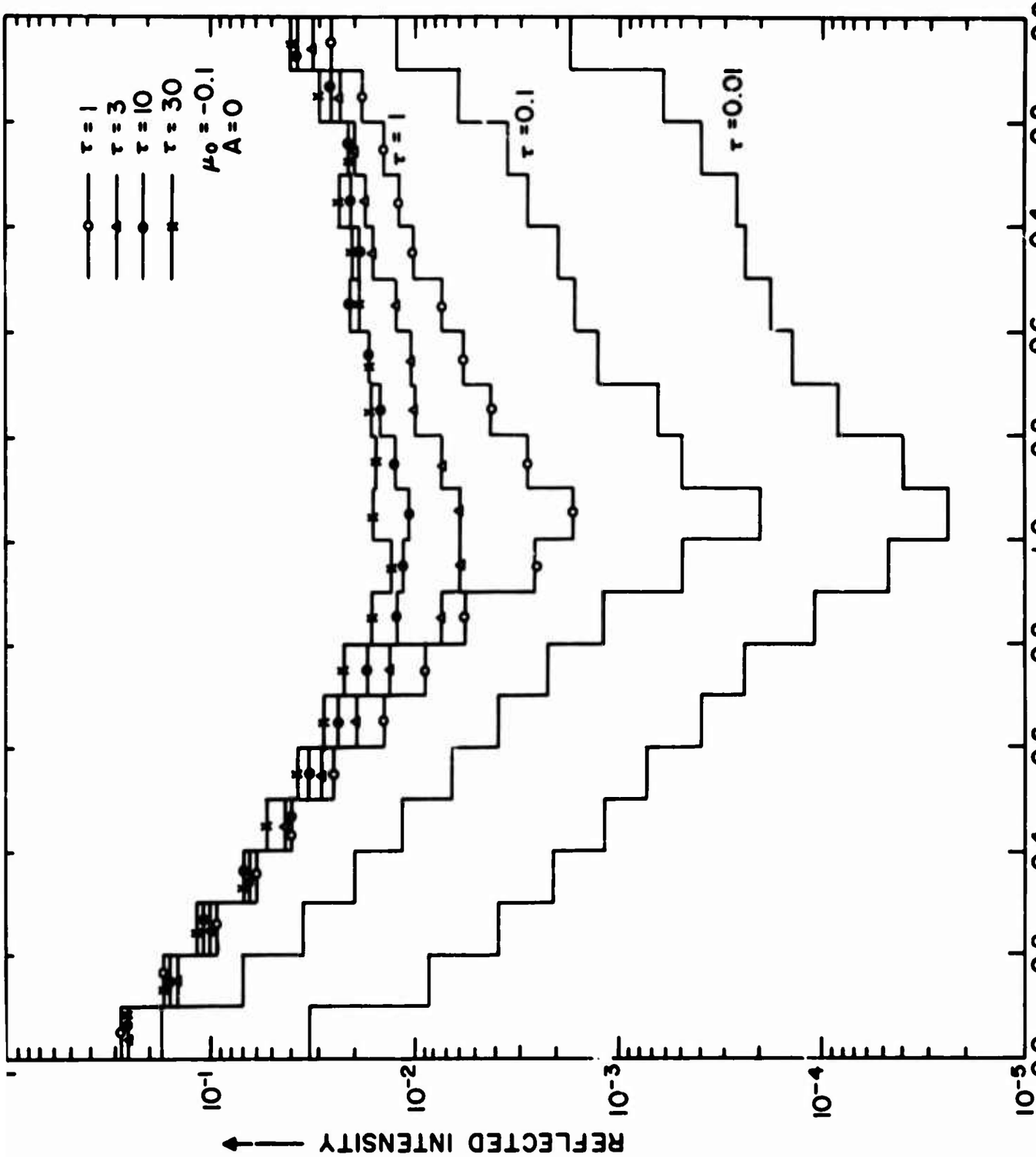
τ = 1
τ = 3
τ = 10
τ = 30
μ0 = -0.1
A = 0
τ = 1
τ = 0.1
τ = 0.01
REFLECTED INTENSITY
10-1
10-2
10-3
10-4
10-5
0.0
0.2
0.4
0.6
0.8
1.0
0.8
0.6
0.4
0.2
0.0
μ

FIGURE 10

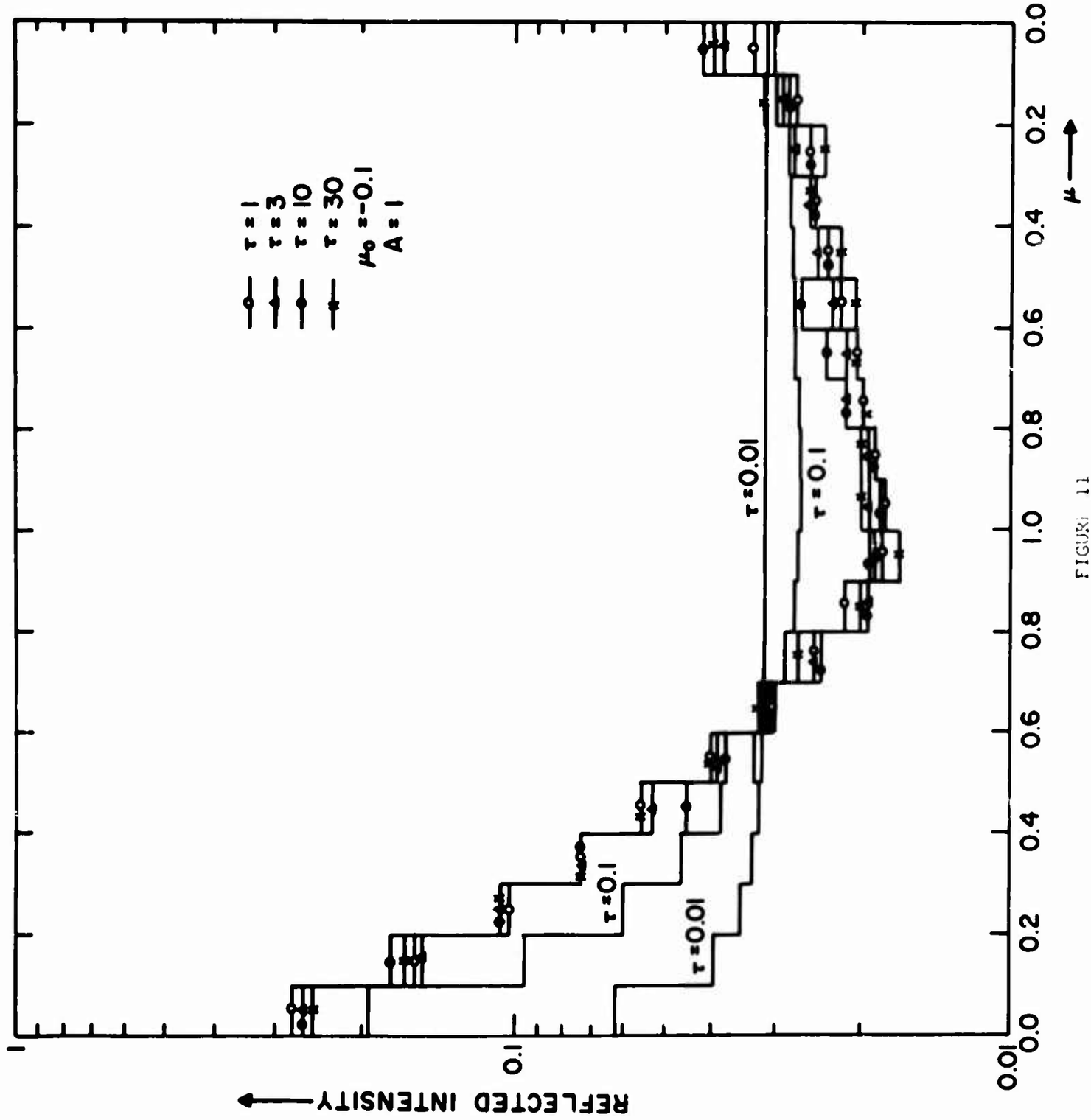
τ = 1
τ = 3
τ = 10
τ = 30
μ₀ = -0.1
A = 1
τ = 0.01
τ = 0.1
τ = 0.01
τ = 0.1
REFLECTED INTENSITY
1.0
0.1
0.01
0.0
0.2
0.4
0.6
0.8
1.0
0.8
0.6
0.4
0.2
0.0
μ

FIGURE 11

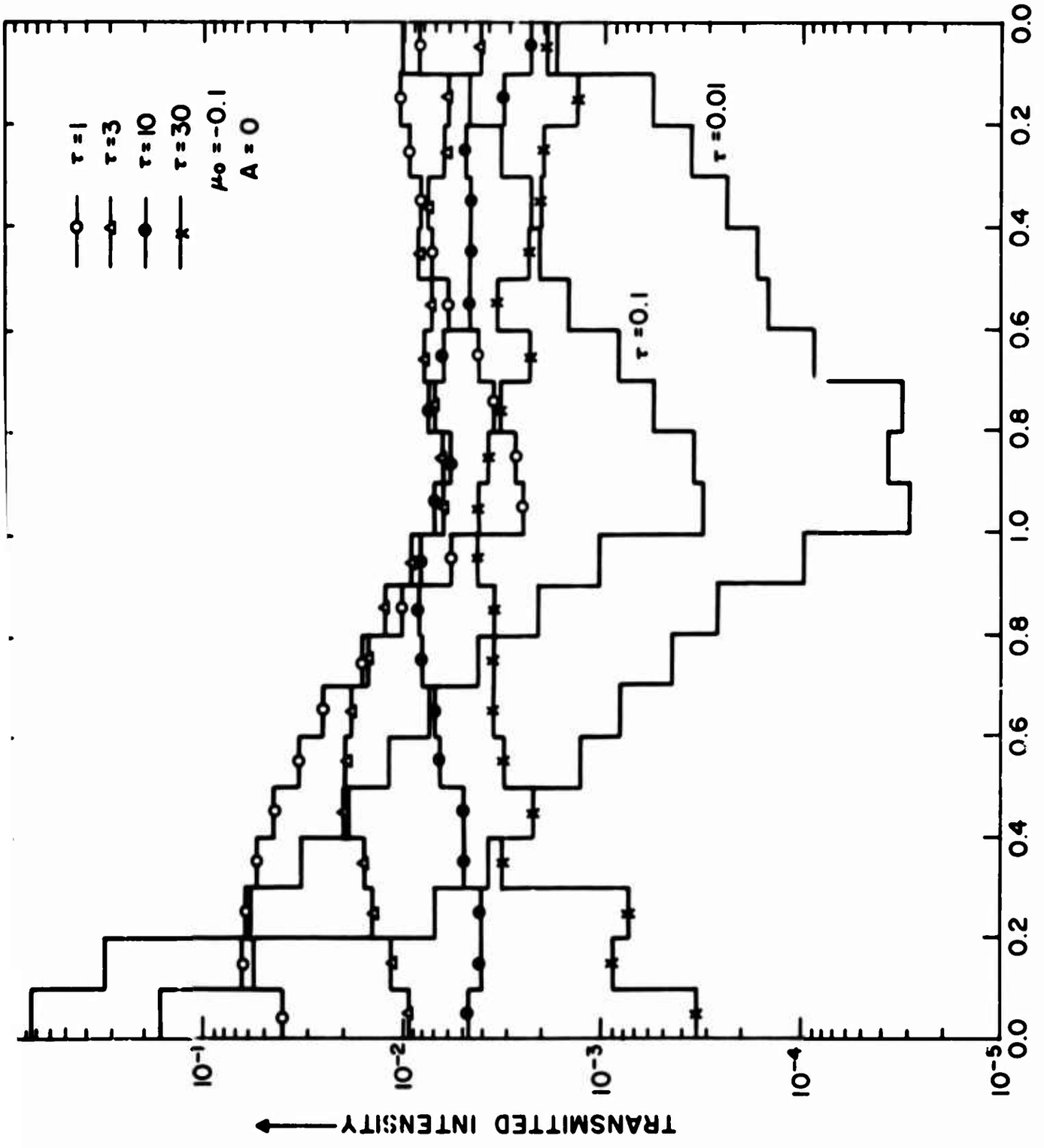
τ=1
τ=3
τ=10
τ=30
μ₀=-0.1
A=0
τ=0.01
τ=0.1
TRANSMITTED INTENSITY
μ
0.0
0.2
0.4
0.6
0.8
1.0
10⁻¹
10⁻²
10⁻³
10⁻⁴
10⁻⁵

FIGURE 12

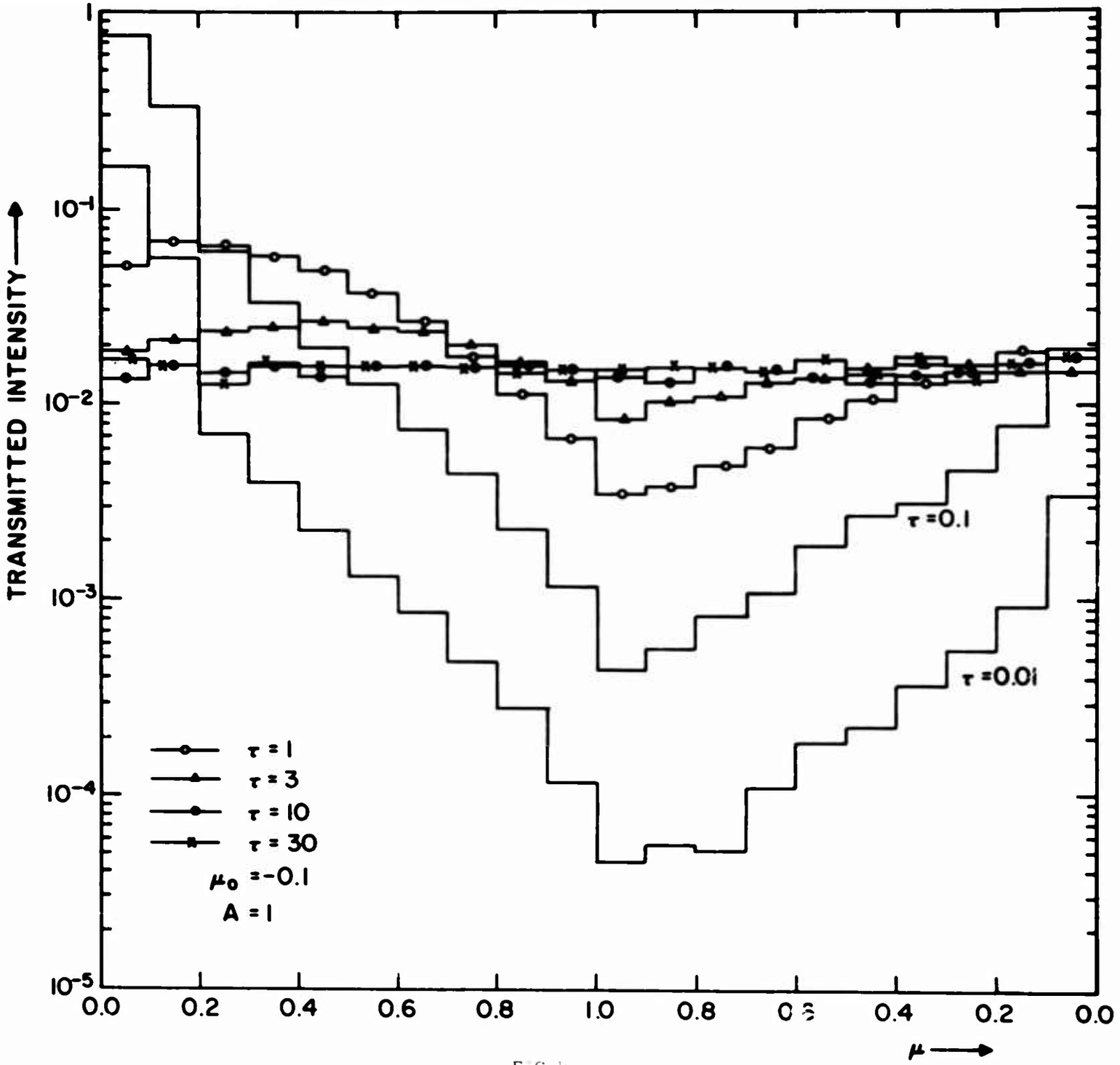
TRANSMITTED INTENSITY
1
10^{-1}
10^{-2}
10^{-3}
10^{-4}
10^{-5}
0.0
0.2
0.4
0.6
0.8
1.0
0.8
0.6
0.4
0.2
0.0
μ
τ = 1
τ = 3
τ = 10
τ = 30
μ_0 = -0.1
A = 1
τ = 0.1
τ = 0.01

FIG.

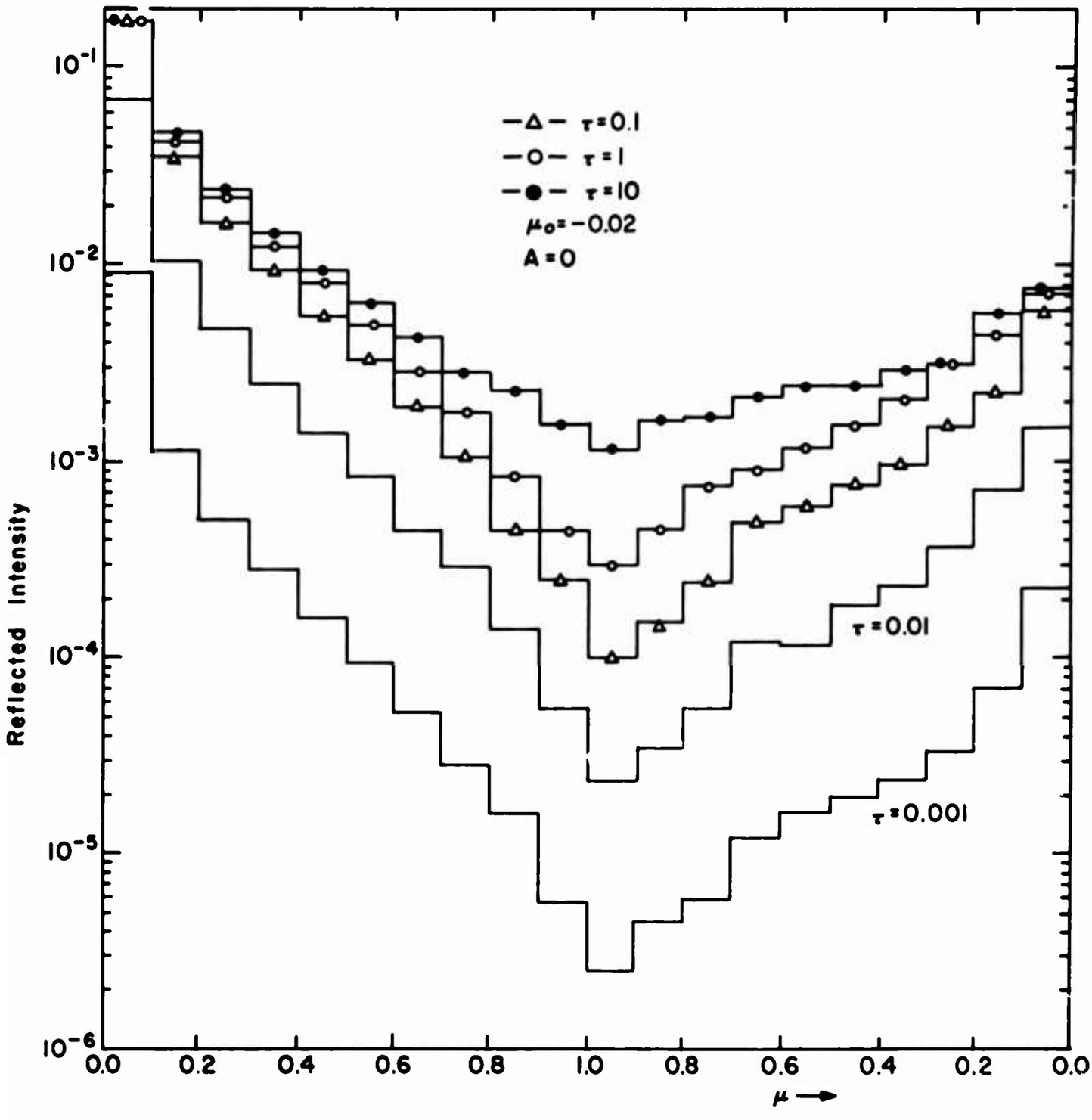
Reflected Intensity
10^{-1}
10^{-2}
10^{-3}
10^{-4}
10^{-5}
10^{-6}
—Δ— τ=0.1
—○— τ=1
—●— τ=10
μ_o=-0.02
A=0
τ=0.01
τ=0.001
0.0 0.2 0.4 0.6 0.8 1.0 0.8 0.6 0.4 0.2 0.0
μ →

FIGURE 14

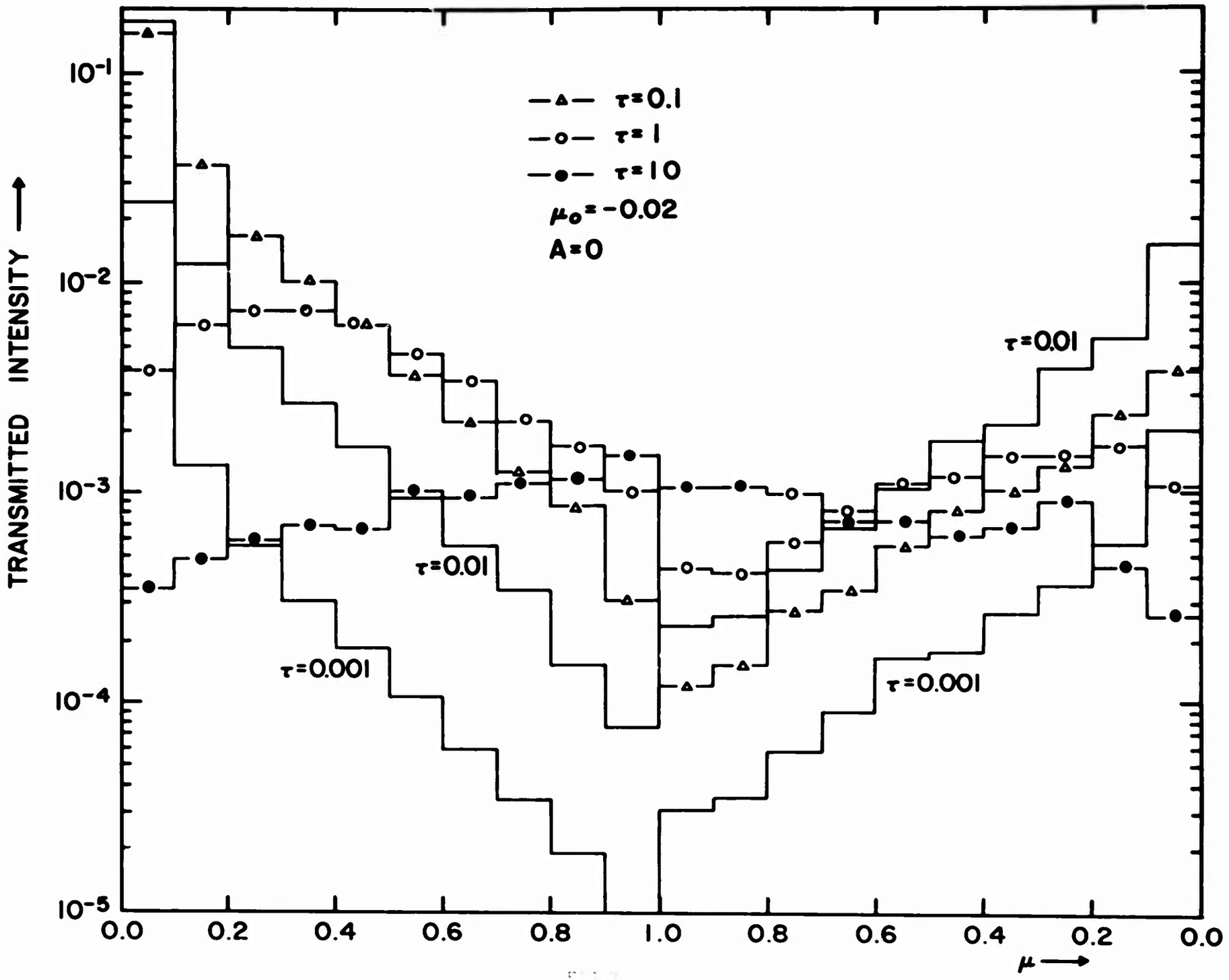
—△— τ=0.1
—○— τ=1
—●— τ=10
μ₀=-0.02
A=0
τ=0.01
τ=0.01
τ=0.001
τ=0.001
TRANSMITTED INTENSITY
10⁻¹
10⁻²
10⁻³
10⁻⁴
10⁻⁵
0.0
0.2
0.4
0.6
0.8
1.0
0.8
0.6
0.4
0.2
0.0
μ

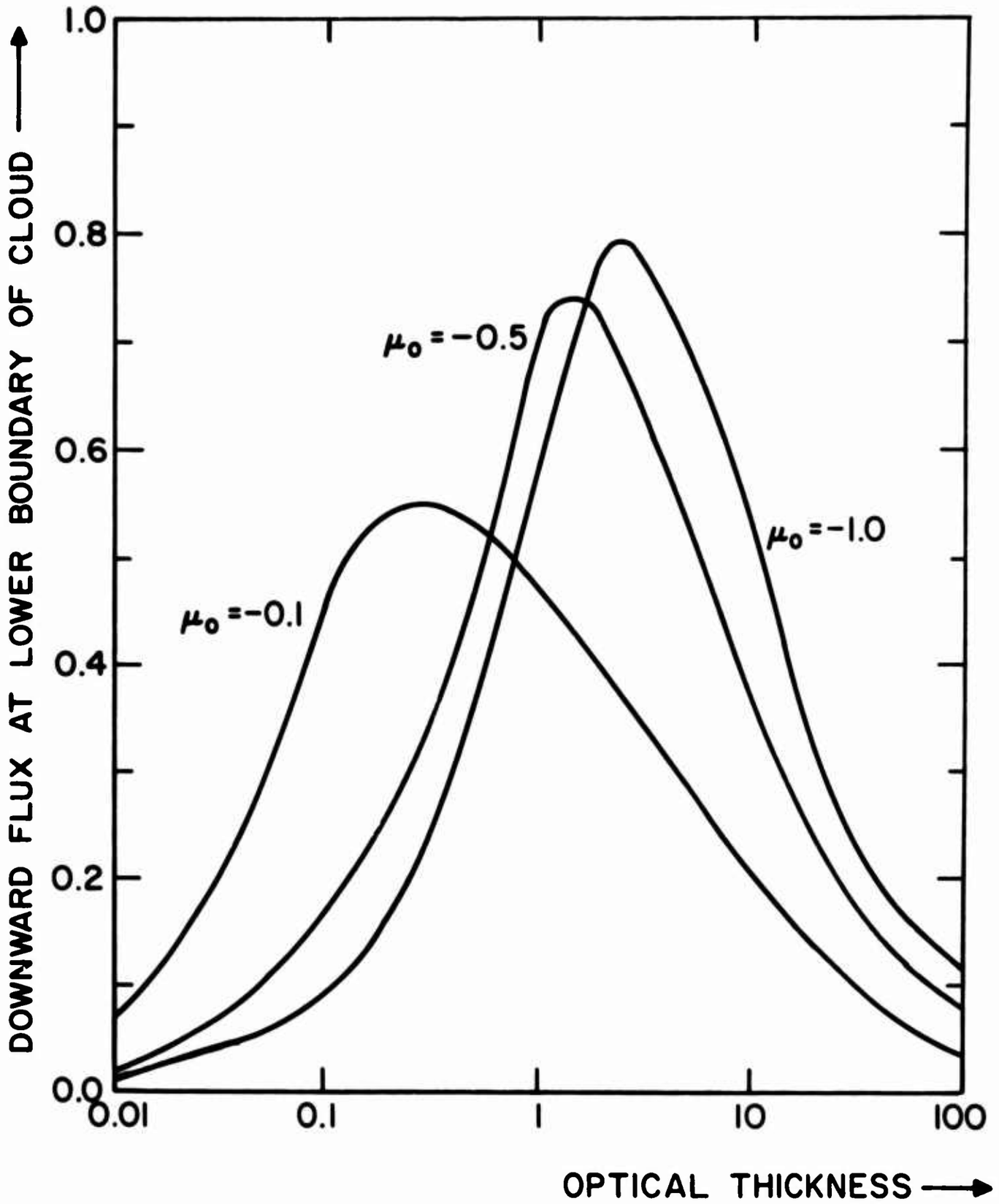
DOWNWARD FLUX AT LOWER BOUNDARY OF CLOUD
1.0
0.8
0.6
0.4
0.2
0.0
0.01
0.1
1
10
100
OPTICAL THICKNESS
$\mu_0 = -0.5$
$\mu_0 = -1.0$
$\mu_0 = -0.1$

FIGURE 15

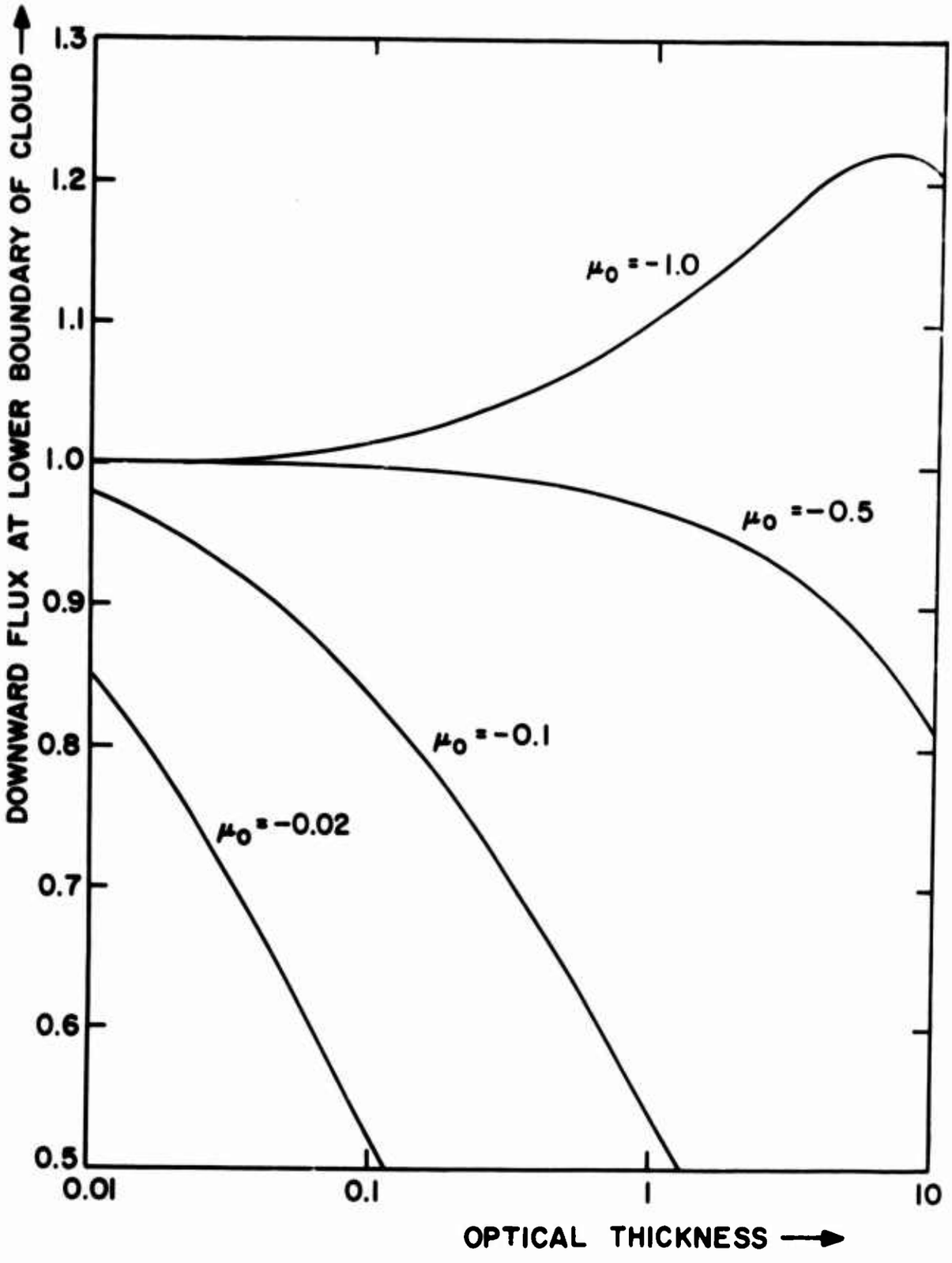
DOWNWARD FLUX AT LOWER BOUNDARY OF CLOUD
1.3
1.2
1.1
1.0
0.9
0.8
0.7
0.6
0.5
$\mu_0 = -1.0$
$\mu_0 = -0.5$
$\mu_0 = -0.1$
$\mu_0 = -0.02$
0.01
0.1
1
10
OPTICAL THICKNESS

FIGURE 17

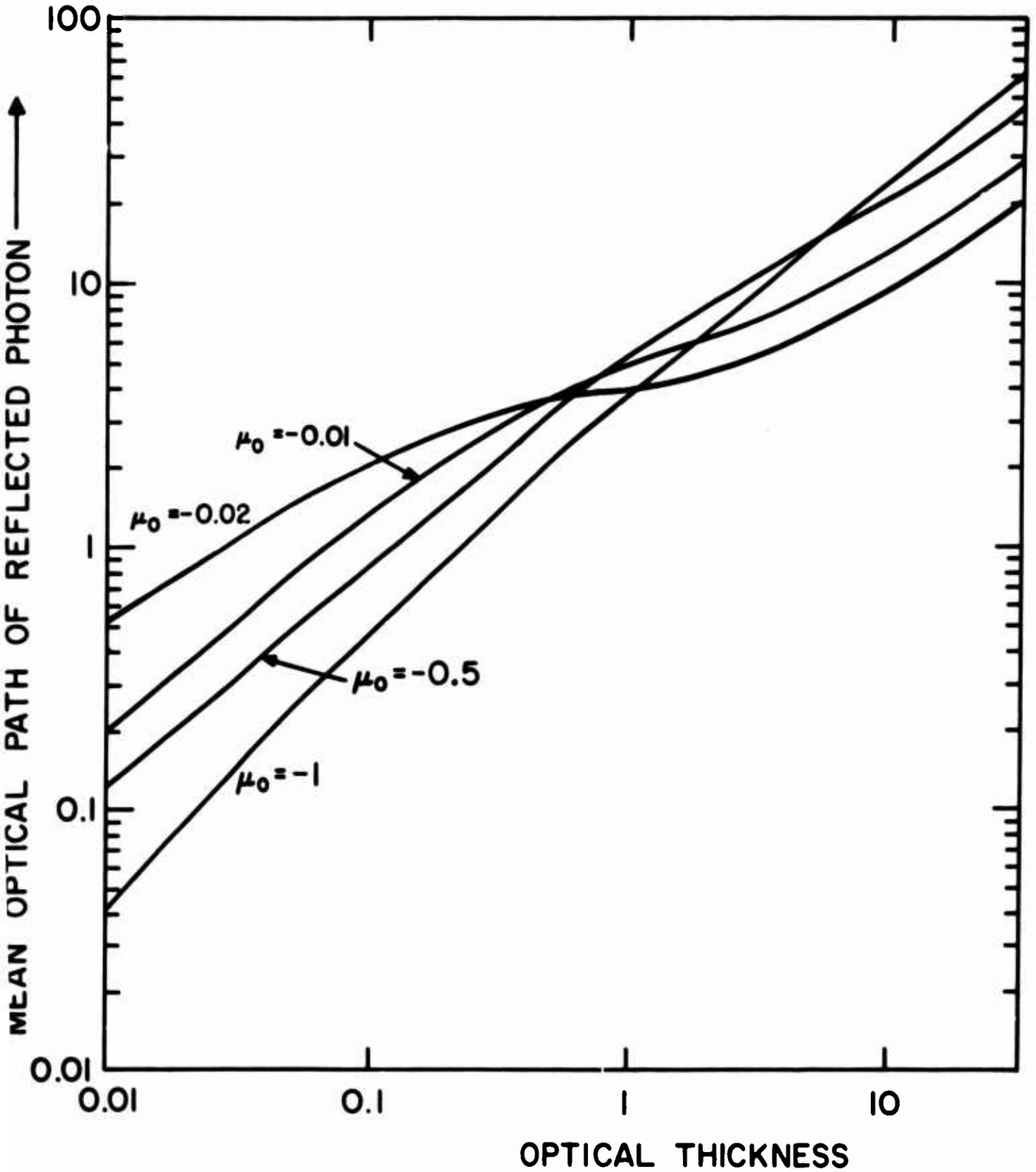
100
10
1
0.1
0.01
0.01
0.1
1
10
MEAN OPTICAL PATH OF REFLECTED PHOTON
OPTICAL THICKNESS
μ_0 =-0.01
μ_0 =-0.02
μ_0 =-0.5
μ_0 =-1

FIGURE 18

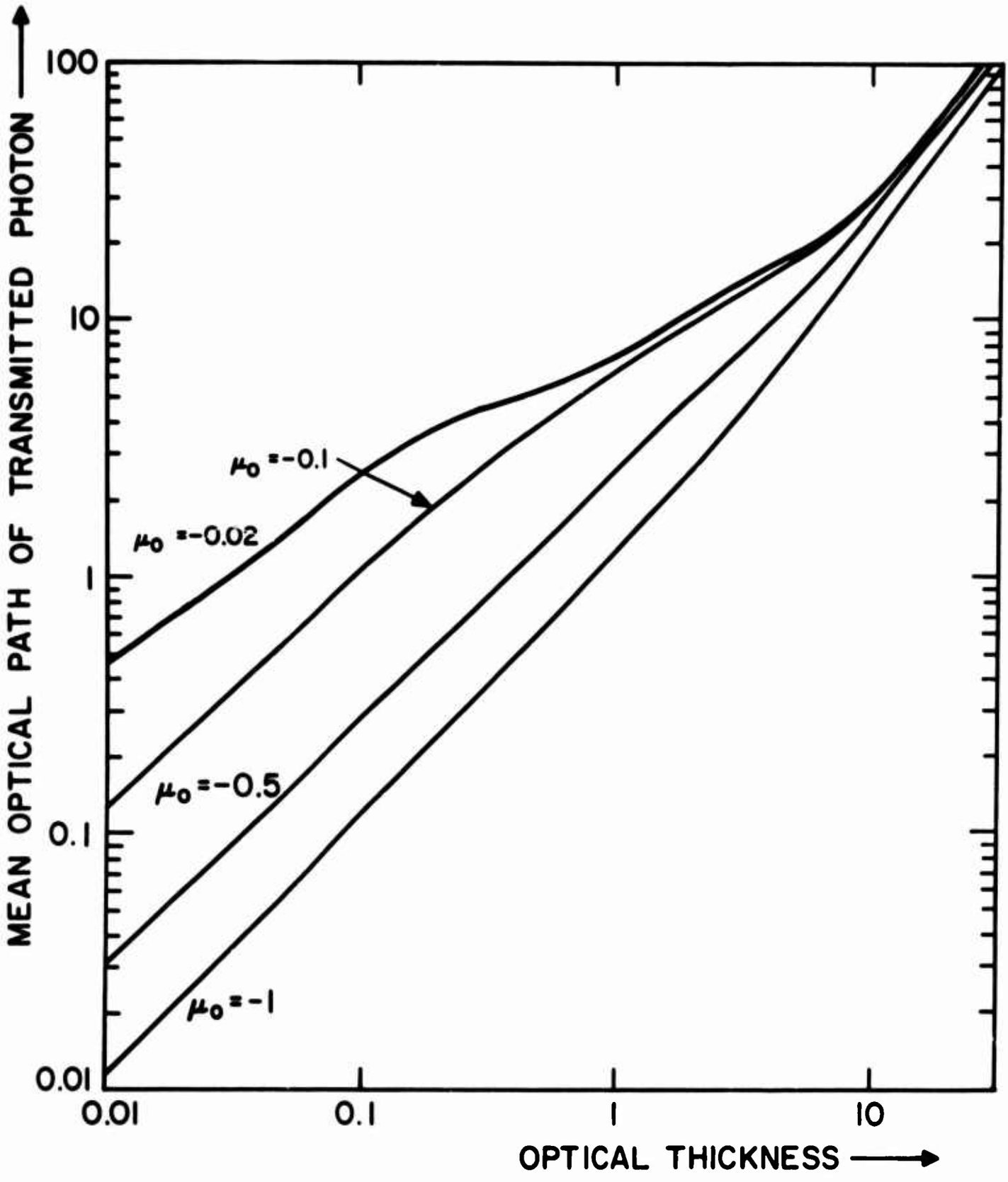
MEAN OPTICAL PATH OF TRANSMITTED PHOTON
100
10
1
0.1
0.01
0.01
0.1
1
10
OPTICAL THICKNESS
μ0 =-0.1
μ0 =-0.02
μ0 =-0.5
μ0 =-1

FIGURE 19

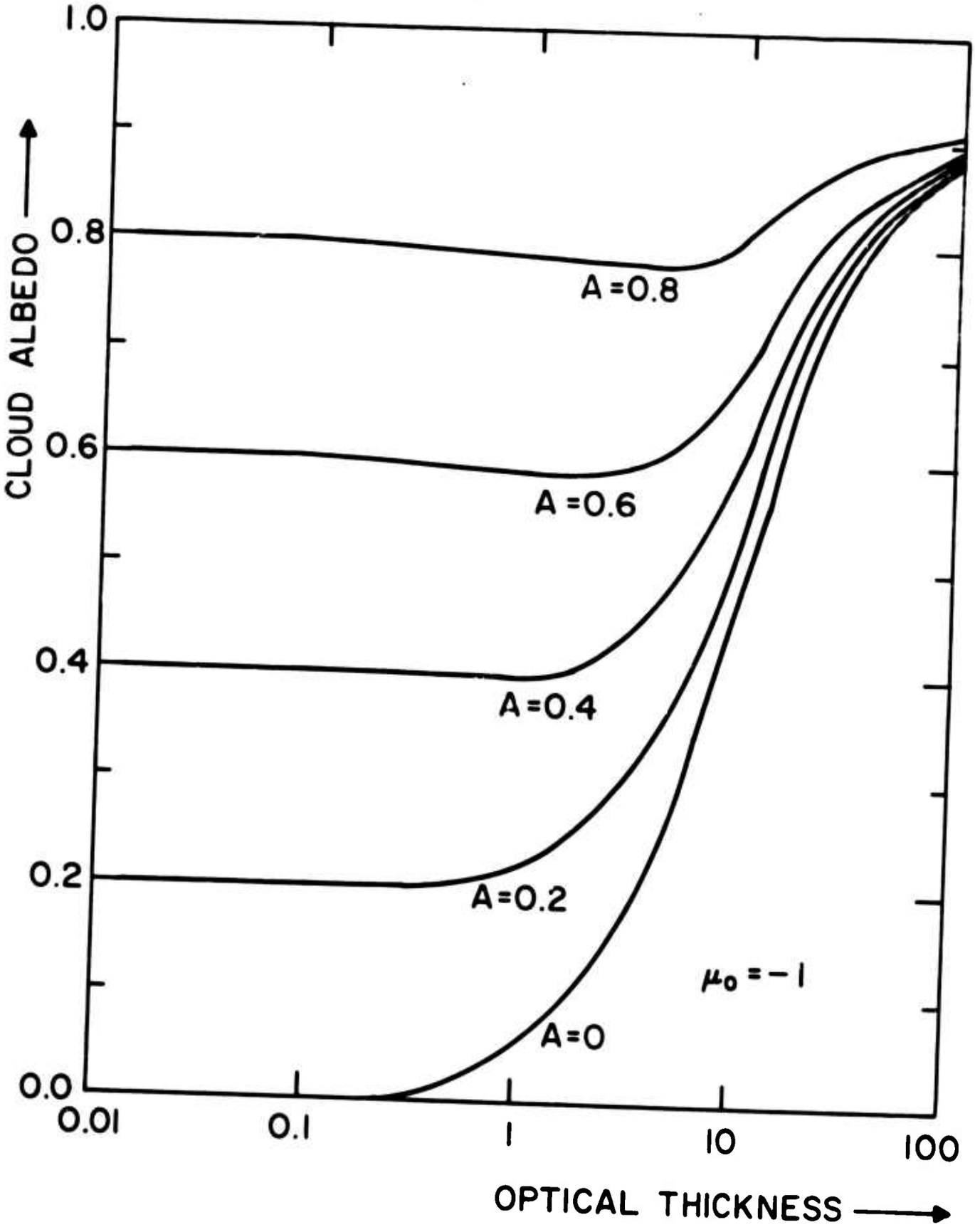
1.0
0.8
0.6
0.4
0.2
0.0
CLOUD ALBEDO
A=0.8
A=0.6
A=0.4
A=0.2
A=0
$\mu_0 = -1$
0.01
0.1
1
10
100
OPTICAL THICKNESS

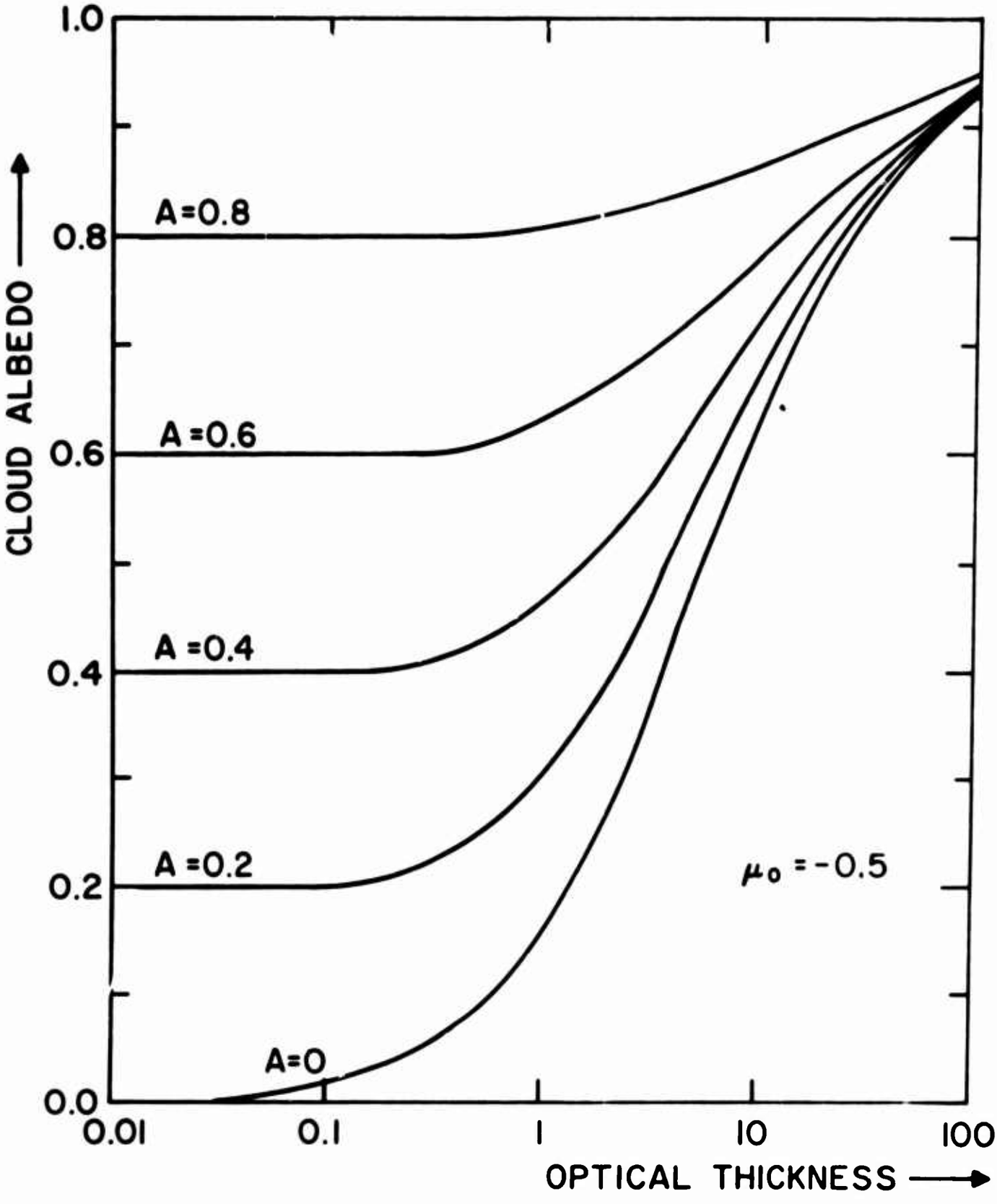
1.0
0.8
0.6
0.4
0.2
0.0
CLOUD ALBEDO
A=0.8
A=0.6
A=0.4
A=0.2
A=0
$\mu_0 = -0.5$
0.01
0.1
1
10
100
OPTICAL THICKNESS

FIGURE 21

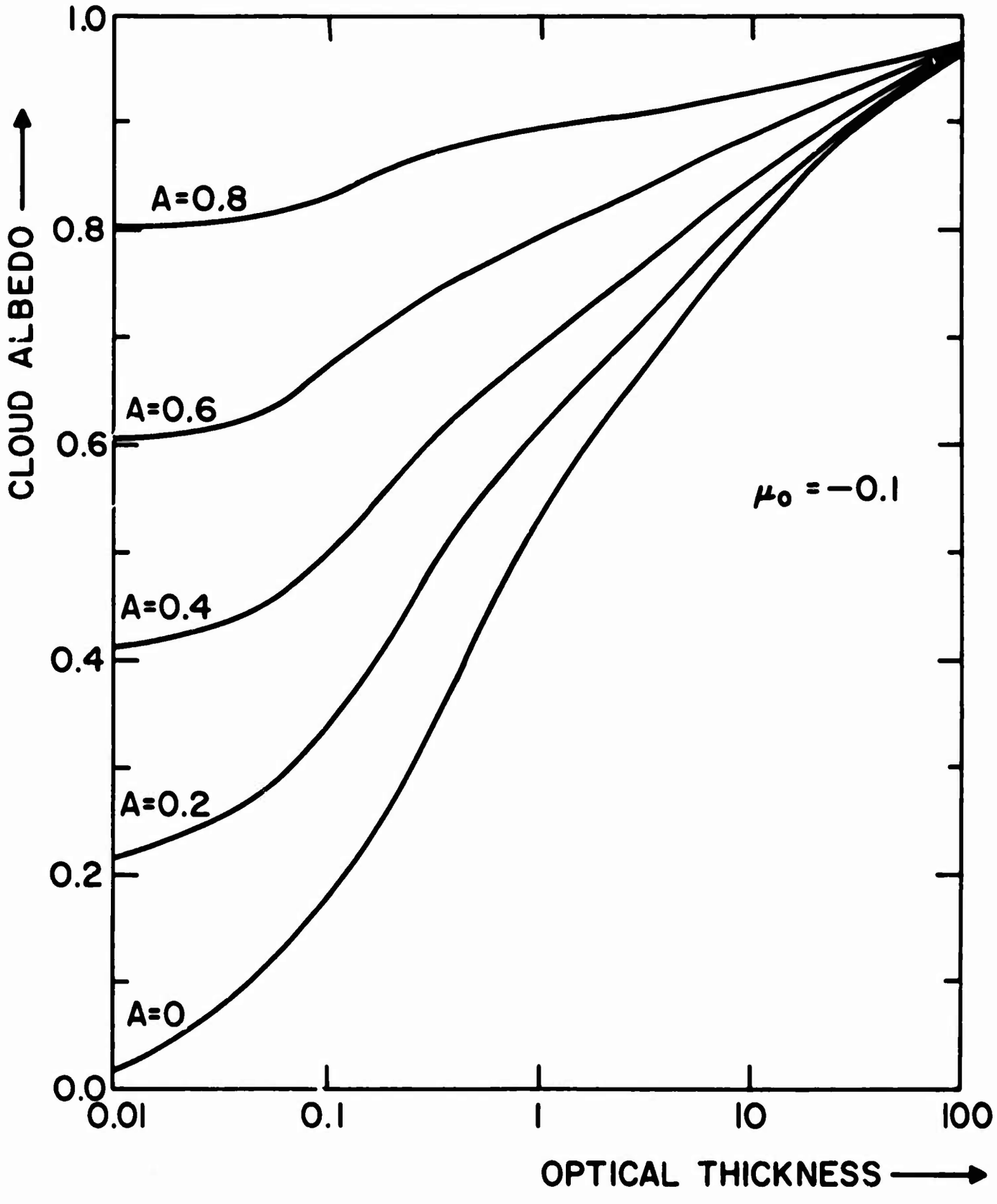
1.0
0.8
0.6
0.4
0.2
0.0
CLOUD ALBEDO
A=0.8
A=0.6
A=0.4
A=0.2
A=0
$\mu_0 = -0.1$
0.01
0.1
1
10
100
OPTICAL THICKNESS

FIGURE 22

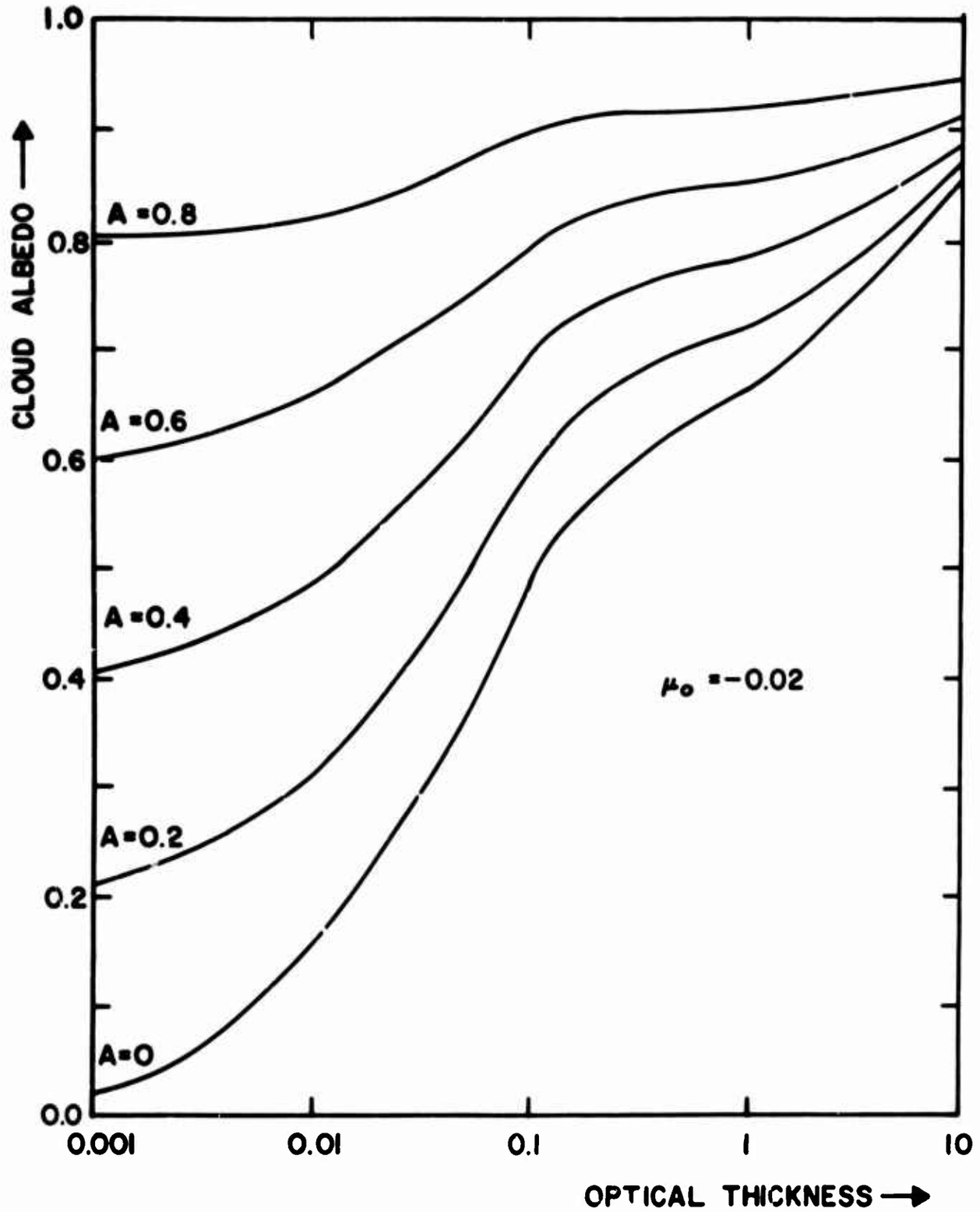
1.0
0.8
0.6
0.4
0.2
0.0
CLOUD ALBEDO
A =0.8
A =0.6
A =0.4
A=0.2
A=0
μ_o =-0.02
0.001
0.01
0.1
1
10
OPTICAL THICKNESS

FIGURE 13

Unclassified
Security Classification

DOCUMENT CONTROL DATA - R & D

(Security classification of title, body of abstract and indexing annotation must be entered when the overall report is classified)

1. ORIGINATING ACTIVITY (Corporate author) Southwest Center for Advanced Studies Dallas, Texas 75230	2a. REPORT SECURITY CLASSIFICATION Unclassified 2b. GROUP

3. REPORT TITLE

MONTE CARLO CALCULATIONS OF LIGHT SCATTERING FROM CLOUDS

4. DESCRIPTIVE NOTES (Type of report and inclusive dates)
Interim Scientific Report

5. AUTHOR(S) (First name, middle initial, last name)

Gilbert N. Plass
George W. Kattawar

6. REPORT DATE	7a. TOTAL NO. OF PAGES	7b. NO. OF REFS
23 May 1967	46	10

8a. CONTRACT OR GRANT NO AF19(628)-5039 b. PROJECT NO 4076- 04 62405484 c 634076	9a. ORIGINATOR'S REPORT NUMBER(S) Scientific Report No. 2 9b. OTHER REPORT NO(S) (Any other numbers that may be assigned this report) AFCRL-67-0421

10. DISTRIBUTION STATEMENT

Distribution of this document is unlimited. It may be released to the Clearinghouse, Department of Commerce, for sale to the general public.

11. SUPPLEMENTARY NOTES	12. SPONSORING MILITARY ACTIVITY Air Force Cambridge Research Laboratories (CRO), L. G. Hanscom Field Bedford, Massachusetts 01730

13. ABSTRACT

The scattering of visible light by clouds is calculated from an efficient Monte Carlo code which follows the multiply scattered path of the photon. The single scattering phase function is obtained from the Mie theory by integration over a particle size distribution. The photons are followed through a sufficient number of collisions and reflections from the lower surface (which may have any desired albedo) until they make a negligible contribution to the intensity. Various variance reduction techniques were used to improve the statistics. The reflected and transmitted intensity is studied as a function of solar zenith angle, optical thickness, and surface albedo. The downward flux, cloud albedo, and mean optical path of the transmitted and reflected photons are given as a function of these same parameters. The numerous small angle scatterings of the photon in the direction of the incident beam are followed accurately and produce a greater penetration into the cloud than is obtained with a more isotropic and less realistic phase function.

DD FORM NOV 1473

Unclassified
Security Classification

Unclassified

Security Classification

14 KEY WORDS	LINK A		LINK B		LINK C	
	ROLE	WT	ROLE	WT	ROLE	WT
Monte Carlo Calculations						
Multiple Scattering						
Clouds						
Reflected and Transmitted Light						

Unclassified

Security Classification